PART - B

CHAPTER - IX

PROTON CONDUCTING STUDY OF POLY (GLYCEROL SUBERATE) POLYESTER (PGSU) - PVA BLEND POLYMER ELECTROLYTE WITH NH_4SCN FOR ENERGY STORAGE DEVICES

9.1 INTRODUCTION

Life seems to be undesirable without the usage of electronic gadgets whose life span is decided by the performance of batteries embedded. The extent of a battery can be predicted from its electrolyte which should fulfil the requirements such as safety, reliability and stability thereby facilitating ion transportation[1,2]. Though the liquid electrolytes were widely used for a long time due to its remarkable ionic conductivity, its risks associated with flammability, volatile nature and leakage[3] has limited its efficiency paving way for solid electrolytes that could be clustered under solid inorganic or polymer electrolyte. Over inorganic solid electrolytes, fast ion conductors (solid polymer electrolyte) is credited as one of the emerging key material in various energy storage devices due to its high flexibility, facile processing and least interfacial hindrance[4].

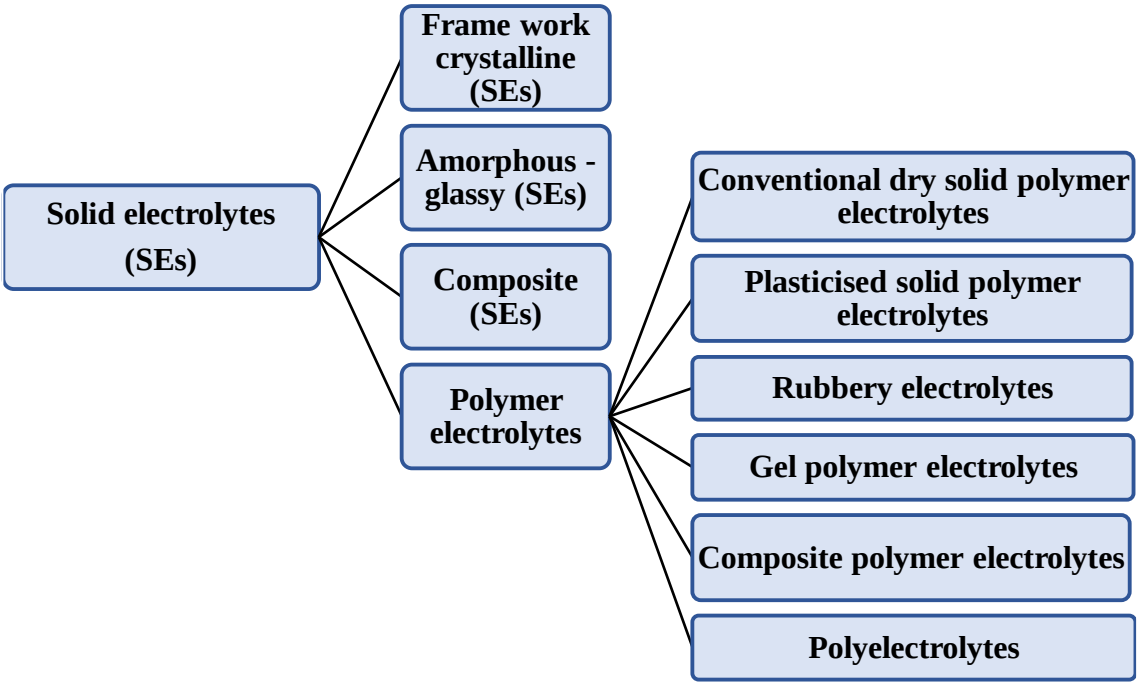

Fig. 1 Classification of solid electrolytes

The transportation of ions in solid electrolytes is validated by the presence of crystal structure, lattice arrangement, concentration of mobile ions, size, polarisability pathway and interaction of ions with supporting matrix. Based on these physical properties the solid electrolytes can be classified according to the chart[5] represented in **Fig. 1**.

Out of the above classification, polymer electrolytes incorporated with fascinating properties like film forming ability, thermal and mechanical stability has deserved its uniqueness forever. The following detailed insight elaborates the various forms of polymer electrolytes as represented in the chart.

(i) Conventional dry solid polymer electrolytes

It favours the formation of polymer complexes where a desired amount of ion donating salts are dissolved in high molecular weight polymeric hosts such as polyethylene oxide (PEO), polypropylene oxide (PPO), polyvinyl pyrrolidine (PVP), poly(vinyl alcohol) whose ionic transportation is facilitated by its amorphous nature, local relaxation and segmental motion of the polymers[6].

(ii) Plasticized solid polymer electrolytes

Plasticising process arises when there is a need to suppress the semi-crystalline (or) crystalline nature of the host polymer which is a key factor in reducing ionic conductivity. This is attained by adding liquid plasticisers like low molecular weight poly(ethylene glycol) (PEG) or aprotic organic solvents like ethylene carbonate (EC), propylene carbonate (PC), diethylene carbonate (DEC) or dimethylsulfoxide (DMSO) into dry solid polymer electrolyte (SPE) matrix which decreases the crystallinity, thereby increasing glass transition temperature and segmental motion, obviously leading to higher ionic conductivity. On the other hand the high dielectric constants of aprotic solvents enhances dissolution of ions rendering more ions in free state responsible for conductivity[7,8].

(iii) Rubbery electrolytes

Rubbery electrolytes are simply polymer -in-salt configuration, where a high molecular weight polymer in minimum level is added to a large amount of salt resulting in a rubbery texture.

(iv) Gel polymer electrolytes (GPEs)

GPEs are generally a continuous existence of liquid phase (org. solvents + plasticizers + ion donating salts) within a solid skeleton of polymer whose conductivity is aided by the presence of large amount of liquid phase. Since its mechanical strength seems to be less, a study on composite polymer electrolytes were made[9].

(v) Composite polymer electrolytes

In order to overcome the drawbacks of GPEs, electrolytes endeavouring high mechanical stability along with good ionic conductivity called as composite polymer electrolytes were studied with minimum amount of ceramic fillers like SiO_2, $BaTiO_3$ or Al_2O_3 dispersed in GPEs[10-12].

(vi) Polyelectrolytes

Polyelectrolytes are one of the major class of emerging electrolytes that possess ion generating groups in its back bone. Its remarkable achievement is reflected in the form of nafion membrane which has its foot print in fuel cell applications[13] due to its high mechanical and chemical stability, exhibiting high ionic conductivity.

9.1.1 Criteria for a polymer electrolyte

Most of the solid polymer electrolytes exhibit the following properties such as

- Chemical and electrochemical stability
- Good mechanical strength
- Facile processing
- No ease of leakage
- Flexible nature
- Non-volatile
- Possible extent of conductivity

9.1.2 Applications of polymer electrolytes

At the time of inception of polymers in the mid of 1970s, less cost effectiveness was noticed which shifted the research towards the findings of high performance materials. It was a duration where the ideas were to be rationalised for further proceedings. This indeed made a platform for the researchers with emerging multidisciplinary thoughts of diversified fields.

Such scientific community gained considerable attention when the applications of polymers were bought into various fields as represented below,

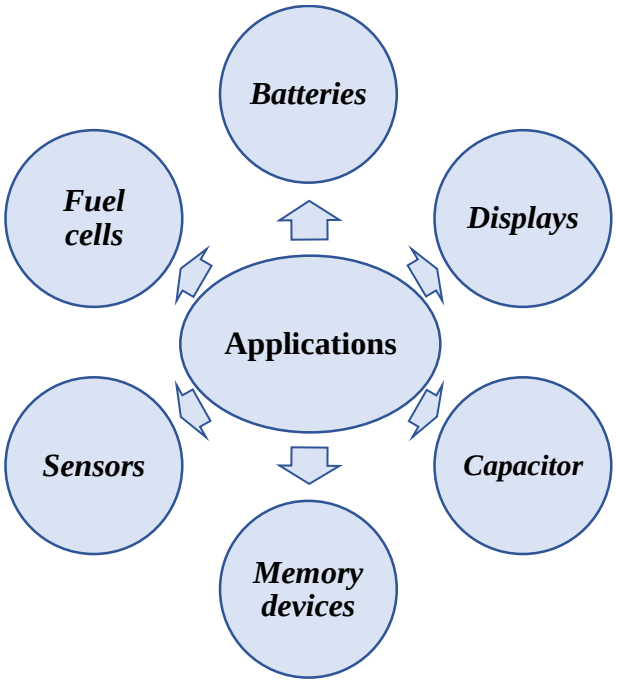

9.1.3 Criteria for formation of Polymer - Salt complex

The following are the basic thumb rules where one can experience a facile complexing ability between polymer and the added salt (dopant).

- Polymers should have low glass transition temperature (T_g)
- Flexible back bone of polymeric system
- Priority to the polymers of low cohesive energy
- Sufficient concentration of the polar groups
- Less distance between the interacting sites
- Repeating units of the polymer to be as far as possible to bring out free rotation within polymer.

The polymer electrolytes subjected to any of the application should ensure three fundamental requirements like performance, durability and cost. Besides the polymer electrolytes employed should specifically act to,

(i)separate two electrodes

(ii)provide good electronic insulation

(iii)allow a fast and selective transport of the desired ions

Thus an urge to fabricate good tensile membranes has made to adopt various approaches like cross linking, blending, adding inorganic inert fillers (or) plasticisers as discussed above that can finally lead to enhanced properties which could not be achieved with a single polymer[14]. Though **Fenton *et al.,*** was the first to shape polymer electrolytes in 1973, it was later enlightened by **Armand *et al.,*** in 1978 in the form of low conducting polymer (10^{-8} S/cm) poly (ethylene oxide) (PEO) which led to the successful findings. In specific, the dual role of solid polymer electrolytes both as ion carrier as well as binder between cathode and anode[15] has made ample researchers to fleet towards finding new polymeric materials. As a motto of finding a new material, polymer blend was preferably chosen because of its ease in physically blending two structurally different polymers that can interact through the secondary forces, becoming miscible at molecular level with controlled physical properties which determined the polymeric film properties[16]. With a spark of this idea, the present discussion has involved poly(vinyl alcohol) (PVA), a semi crystalline, non-toxic, eco-friendly primary synthetic polymer[17] as a base containing –OH groups in its back bone and poly(glycerol suberate) polyester (PGSU), a biodegradable polymer (synthesis described in chapter II) to get blended, where hydrogen bonding assisted the moulding of a thin film (electrolyte) and its application in proton conducting batteries. The structure of the polymers involved are shown below.

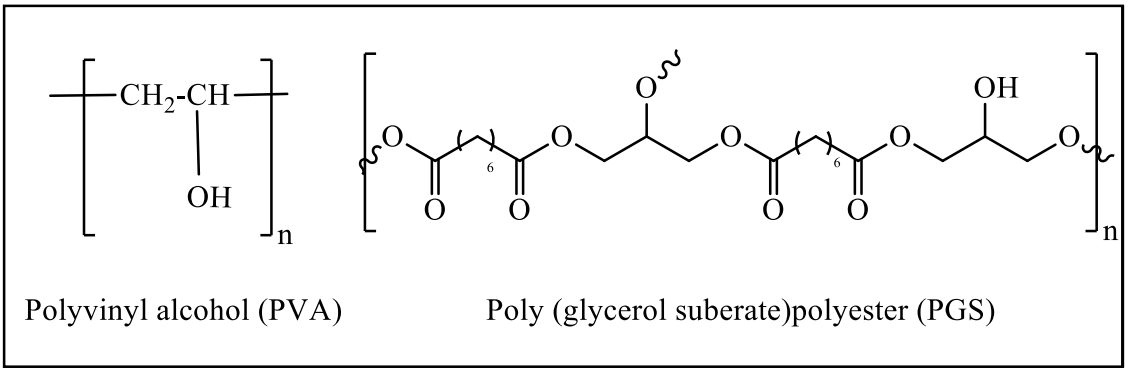

Polyvinyl alcohol (PVA) Poly (glycerol suberate)polyester (PGS)

9.1.4 Review of literature

The following are the reviews representing the electrolytes based on PVA blended with commercially available polymers and its applications in various energy storage devices which could form a base line for the present discussion.

Savitha Thayumanasundaram *et al.,* blended 25 mol % poly (acrylic acid) and 75 mol % poly(vinyl alcohol) with 1-butyl-1-methylpyrrolidinium bis(trifluoro methane sulfonyl) imide and 0.2 M lithium bis(trifluoromethansulfonyl)imide. By varying the concentrations of

ionic liquid, it was optimised at 70 mol% with a conductivity of 1 mS cm^{-1}. High reversible redox reactions were evident from cyclic voltammetry studies. Linear sweep voltammetric study suggested this electrolyte for batteries as cathodic material[18].

Manjuladevi *et al.*, successfully applied an electrolyte for magnesium battery by mixing poly(vinyl alcohol) and polyacrylonitrile in the ratio 92.5:7.5 along with $Mg(ClO_4)_2$ using solution cast technique. FT-IR and XRD analysis were carried out to evaluate the extent of salt blended. Using AC-impedance spectroscopy maximum conductivity of 2.96×10^{-4} S/cm was observed for 0.25 mm% of magnesium salt incorporated electrolyte. Along with the measurement of transference number, primary magnesium battery was constructed and its discharge characteristics were studied[19].

As per the report given by **Alakanandana *et al.*,** the dc conductivity of electrolytes of poly(vinyl alcohol) (PVA) was successively increased when it was blended with poly(vinyl alcohol) by means of solution cast technique. FT-IR and XRD studies revealed the effect of dopant with the polymer and its complexation nature was also elicited[20].

Muthuvinayagam *et al.*, reported a proton conducting blend made from poly(vinylidene fluoride) and poly (vinyl alcohol) along with various concentrations of ammonium thiocyanate. Polymer salt interaction was revealed from FT-IR and DSC techniques which showed a shift in glass transition values. Followed by the determination of amorphous nature from XRD, the surface study was carried out by SEM analysis. Successive increase in ionic conductivity was observed with increase in salt concentration within a range of 10^{-9} to 10^{-3} S/cm [21].

Using facile, eco-friendly method **Md-Jamal Uddin *et al.*,** prepared a separator by blending lignin and poly(vinyl alcohol) in water medium. The membrane resulted was with good compatibility, wettability, thermal stability and flame retarding property. It was concluded that the high porous structure and high ionic conductivity of the electrolyte prepared can be applied as a safer separator for lithium batteries[22].

Chun-ChenYang developed an alkaline polymer electrolyte using poly(vinyl alcohol) (PVA) with polyethylene oxide (PEO) whose ionic conductivity was increased from 10^{-7} to 10^{-2} S cm^{-1}. The activation energy observed was in the range of 3–8 kJ mol^{-1}. Its good stability and high ionic conductivity was examined by various techniques and it was applied as electrolyte film for nickel–metal-hydride (Ni–MH) batteries[23].

Ma *et al.,* revealed the effect of montmorillonite in the composite prepared from nanoclay fillers, lithium-bis(trifluoromethanelsulfonyl) (LiTFSI), polyvinylidene difluoride (PVDF) and poly(vinyl alcohol) (PVA). Highest ionic conductivity with a transference number of 0.4 was recorded for 4 wt % of montmorillonite. Further its good performance evaluated from electrochemical study suggested this composite material to be an apt one for lithium ion batteries[24].

Jhunu Chatterjee *et al.,* utilised N-methyl-2-pyrrolidone as solvent to synthesise poly(vinyl alcohol) (PVA) based polymer electrolyte and explored its application in capacitors as well as batteries. A conductivity of 2×10^{-3}–5.8×10^{-4} S/cm was observed at room temperature. With the aid of carbon nanotube films as active electrodes, specific capacitance of a capacitor was also predicted[25].

A facile fabrication of polymer electrolyte using poly(methyl acrylate-co-acrylonitrile)/ poly (vinyl alcohol) was reported by **Xianguo Ma *et al.,*** in which poly(vinyl alcohol) served as a stabilising agent in providing strength to the polymeric backbone. The synthesised polymer electrolyte was self - standing and mechanically stable with ionic conductivity of 0.98 mS cm^{-1}. Satisfactory compatible results were obtained when it was subjected for Li-ion batteries[26].

An investigation on the dielectric properties of the polymer electrolytes prepared from poly(vinyl alcohol) (PVA), polyethylene glycol (PEG) and ammonium thiocyanate (NH_4SCN) was made by **Arvind Awadhia *et al.,*** with a temperature and frequency lying in the range of 273–373 K and 40 Hz–100 KHz. The time of relaxation observed for conductivity (σ), segmental (α) and dipolar (β) motion was found to obey Arrhenius equation associated with low energy of activation compared to PVA–NH_4SCN complexes in the absence of solvent[27].

Nilesh R. Chodankar *et al.,* studied the effect of the polymer gel electrolytes such as poly(vinyl alcohol) (PVA), carboxymethyl cellulose (CMC) and polyethylene oxide (PEO) on electrochemical performance of MnO_2 - flexible solid state super capacitors (FSS-SCs). From the studies it was revealed that maximum operating potential (1.2 V), energy density (15 W h kg^{-1}), specific capacitance (112 F g^{-1}) and cyclic stability (2500 CV) was favoured by the poly(vinyl alcohol) (PVA)–lithium perchlorate ($LiClO_4$) gel electrolyte followed by a decrease in its efficiency after 20 days[28].

A promising material comprising of polyethylene oxide (PEO), poly(vinyl alcohol) (PVA) and glass-fibre-mat polymer electrolyte was successfully applied as an electrolyte for primary Zn–air batteries by **Chun-Chen Yang *et al.,*** due to its excellent conductivity of

10^{-2} S cm^{-1}. Experimental investigation by means of of ac impedance spectroscopy and galvanostatic discharge revealed its electrochemical characteristics making it suitable for batteries[29].

A novel poly(vinyl alcohol) (PVA) / polyvinyl pyrolidine (PVP) electrolyte membrane was synthesised by **Jinli Qiao *et al.,*** by means of blending, cross linking and doping with KOH. A detailed characterisation was made using FTIR, TG and SEM analysis. The ionic conductivity was found to be influenced mainly by the concentration of KOH where a maximum conductivity of 0.53 S cm^{-1} was favoured by 8 M KOH. SEM analysis revealed uniform distribution whereas FT-IR suggested that the conductivity might be due to the excess free KOH in the polymer matrix. A high stable ionic conductivity for more than a month was also observed[30].

Tamilselvi *et al.,* utilised solution casting method to prepare a polymer electrolyte comprising of poly(vinyl alcohol) (PVA), poly(vinylidene fluoride (PVdF) and lithium triflate ($LiCF_3SO_3$). The ionic conductivity successively increased on increasing the concentration of the salt where a maximum conductivity of 2.7×10^{-3} S cm^{-1} was observed for a composition of 80 PVA+ 20 PVdF + 15 $LiCF_3SO_3$. Influence of temperature on the ionic conductivity of the polymer electrolytes were studied and found that they were in good agreement with Arrhenius equation[31].

Geraldine Merle *et al.,* gave a facile low cost method to synthesise KOH - poly(vinyl alcohol) (PVA) cross linked polymer electrolyte which exhibited high ionic conductivity, chemical and thermal stability depending on the extent of crosslinking done. On subjecting to the alkaline fuel cell, it was associated with an OCV (0.95 V) and current density of 200 mA cm^{-2}. It was expected that on increasing the temperature, there could be an increase in performance[32].

Wu *et al.,* synthesised hydrophilic membrane using poly(vinyl alcohol) (PVA) and poly(acrylic acid) (PAA) by means of solution casting technique and its ionic conductivity measured at room temperature was 0.142–0.301 S cm^{-1}. Excellent electrochemical property was confirmed from the cyclic voltammetric technique done using Zn|SPEM|Zn and Al|SPEM|Al cells[33].

Qiumei Wu *et al.,* designed a novel composite material by blending a mixture of PVA, TiO_2, KOH, and H_2O. The membrane synthesised was analysed using DSC and XRD which revealed that the amorphous hump of PVA matrix was suppressed due to the addition of TiO_2.

SEM analysis confirmed the dispersion of TiO_2 within the matrix. On evaluating its electrochemical properties, ionic conductivity between 0.102 and 0.171 S cm^{-1} was observed at room temperature which made it to behave as an excellent candidate for Zn–Ni secondary battery with low redox reactions[34].

Saroj *et al.,* paved a method of synthesising electrolytes by varying the weight % of 1-ethyl-3-methylimidazolium ethylsulfate (ionic liquid) along with PVA and $LiClO_4$ (15 wt%). XRD and DSC analysis showed an increased amorphous nature on increasing the weight % of ionic liquid. Study on conductivity measurements favoured higher ionic conductivity[35].

A free radical polymerisation was adopted by **Wu *et al.,*** to develop solid polymer electrolyte using poly (vinyl alcohol) (PVA) and poly (acrylic acid) (PAA). The alkaline solid polymer obtained by immersing in 32 wt% of KOH solution was characterised using differential scanning calorimetry (DSC), stress–strain test, X-ray diffraction (XRD) and SEM. Four fold increase in ionic conductivity was observed for PVA/PAA/KOH compared to PVA–KOH electrolyte. Its excellent mechanical, thermal stability and ductility made it as a promising material for electrochemical systems[36].

Chiam-WenLiew *et al.,* developed proton conducting electrolytes by incorporating ionic liquid (1-butyl-3-methylimidazolium chloride (BmImCl)) with poly(vinyl alcohol) (PVA)-ammonium acetate (CH_3COONH_4). With an optimised level of 50 wt% of BmImCl, highest ionic conductivity of 5.74 ± 0.01 mS cm^{-1} was noticed. The stability of the polymer electrolyte was up to 250°C. ATR-FT-IR spectral studies reflected the complexation occurring between PVA, CH_3COONH_4 and BmImCl. At room temperature a maximum power density of 18 mW cm^{-2} was observed for an electrochemical fuel cell[37].

Omed Gh. Abdullah *et al.,* varied the weight % of potassium permanganate to synthesise PVA based electrolyte by solution cast technique. The complexation between PVA and $KMnO_4$ was revealed from FT-IR and XRD analysis. Influence of $KMnO_4$ concentration was clearly predicted from measuring fundamental optical parameters like optical band gap energy, refractive index, optical conductivity and dielectric constants. Optical band gap energy obtained for pure PVA around 6.27 eV was decreased to 3.12 eV when optimised with $KMnO_4$ (4 wt%) salt. Refractive index and dielectric constants calculated for polymer electrolytes was in parallel with $KMnO_4$ content[38].

Study made by **Chiam-Wen Liew *et al.,*** predicted increased ionic conductivity with increase in temperature reaching a maximum of 7.31 ± 0.01 mS cm^{-1} at 120 °C for a system

comprising of poly(vinyl alcohol) (PVA), ammonium acetate (CH_3COONH_4) and 1–butyl–3–methylimidazolium chloride (BmImCl). DSC analysis elicited decreased T_g value when doped with salt. Addition of ionic liquid favoured potent stability. In addition, cyclic voltammetric study, electrochemical impedance and galvanostatic tester gave an energy and power density of 2.39 Wh kg^{-1} and 19.79 W kg^{-1} with 90% coulombic efficiency[39].

Effect of bentonite on poly(vinyl alcohol) (PVA) based alkaline polymer electrolyte was investigated by **Shangbin Sang *et al.,*** who reported breakage of continuous ion conducting phase at low level of KOH and water content followed by an increase in conductivity at higher water content. Maximum conductivity of 0.11 S cm^{-1} was observed at room temperature. Higher temperature studies followed Arrhenius equation with an E_a value of 4 - 6 kJ mol^{-1}. XRD and SEM analysis revealed lot of interspaces pertaining to amorphous structure whose electrochemical stability let it in secondary Zn–Ni cells at low charge–discharge rate[40].

Hamide Aydın *et al.,* synthesised polymer electrolyte by doping the host matrix poly(vinyl alcohol) + poly(ethylene glycol) monomethyl ether + borane–tetrahydrofuran (PVA+PEGME+ BH_3/THF) with CF_3SO_3Li at various proportions. The prepared electrolytes were characterised using ^1H NMR, ^{11}B NMR, FT-IR, TG and DSC. Dielectric impedance spectroscopy was used to measure the ionic conductivity from which $>10^{-4}$ S cm^{-1} conductivity was observed. The electrochemical stability extending over 4V was revealed from cyclic voltammetry[41].

Jak Li *et al.,* incorporated aqueous tetraethyl ammonium hydroxide (TEAOH) into poly(vinyl alcohol) (PVA), polyethylene oxide (PEO) and polyacrylic acid (PAA). Its different performances were revealed clearly using electrochemical impedance spectroscopy and cyclic voltammetry. It was observed that crystallinity, hydrophilicity, functional group and electronegativity of the polymer hosts bought the differences in OH^- ion transportation. From the three polymer electrolytes, TEAOH-PVA and TEAOH-PAA was made suitable for EC applications whose ionic conductivity was 5 mS cm^{-1} with an ultra-high rate of 5000 V/s[42].

From the review of previous work carried out by ample researchers, it can be clearly predicted that the commercially available synthetic polymers has been widely used as solid polymer electrolytes for electrochemical applications. This clearly predicts that work carried on polymers synthesised under lab scale is too scarce which has intended us to take up the present work where the significance of a poly (glycerol suberate) polyester (PGSU) is explored in the form of an electrolyte for battery applications.

9.2 EXPERIMENTAL METHODS

9.2.1 Materials

Poly(vinyl alcohol) (PVA) (Avg. M.wt. 1,25,000), ammonium thiocyanate (NH_4SCN) (M.wt.76.12) were purchased and used as such.

9.2.2 Preparation of Electrolyte film

Poly(vinyl alcohol) (PVA), ammonium thiocyanate (NH_4SCN), synthesised poly (glycerol suberate) (PGSU) were used as precursors. Solution casting technique was adopted to synthesise electrolyte film due to its simplicity compared with other methods. In order to optimise the condition, the work was initiated with a base of 1g PVA as a host polymer. Since the polymer PGSU lacked the tendency to form a free standing film, it was decided to blend with PVA, gradually by raising its proportion likely to be 0.25g, 0.5g and 0.75g and was optimised at a proportion of 1g PVA: 0.75g PGSU. The optimised pure polymer blend was synthesised by dissolving 1g PVA in required amount of water followed by the addition of 0.75g PGSU. By the meantime, various proportions of NH_4SCN (0.5g, 0.6g, 0.7g) were added to the polymeric solution and allowed to stir continuously until a homogeneous mixture was obtained. The solutions were then cast into polypropylene petri dishes and vaccum dried at 60^o until complete removal of moisture was ensured. The obtained free standing films were stored in a desiccator for further proceedings. The schematic representation of film synthesis is shown below in **Fig. 2**.

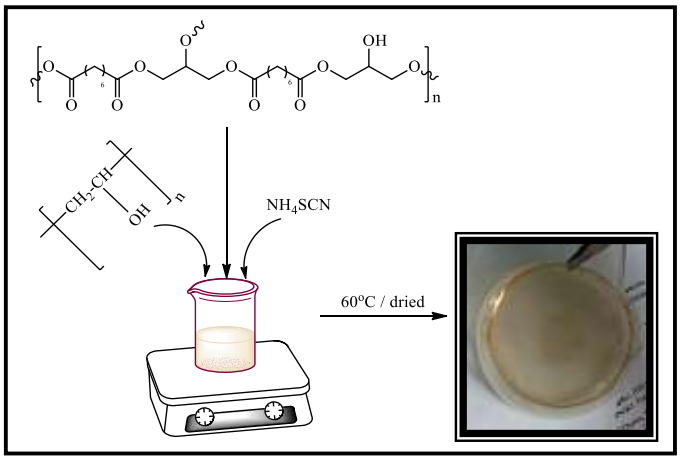

Fig. 2 Synthesis of polymer film

9.2.3 Characterisation techniques

(i) Fourier transform infrared spectroscopy (FT-IR)

With the aid of Schimadzu-ATR-FTIR spectrophotometer, FT-IR spectra of the polymer films were recorded in the range of 4000-400 cm^{-1}.

(ii) X-ray diffraction studies (XRD)

The amorphous or crystalline nature of the synthesised polymer films were assessed from XRD analysis using Rigaku (ULTIMA IV model) X-ray diffractometer within a range of $2\Theta = 10^{o}$ to 90^{o}.

(iii) Differential scanning calorimetry (DSC)

In order to analyse the thermal properties, DSC Q20 was utilised by placing the sample (polymer film) of required amount in an aluminium pan in presence of nitrogen atmosphere with a heat rate of 10^{o} C/min within applied temperature range.

(iv) Scanning electron microscopy (SEM) and Energy dispersive X-ray spectroscopy (EDS)

To analyse the dispersion of dopant within the polymeric backbone, surface examination of prepared membranes were carried out using Nova nano SEM analytical instrument along with the elemental composition from EDS measurements.

9.2.4 Conductivity measurements

9.2.4.1 AC impedance analysis

The polymer electrolytes with and without the dopants of required dimensions were sandwiched between blocking stainless steel electrodes. With an aid of HIOKI 3532 LCR meter Hi-tester, frequency in the range of 42 to 1MHZ was applied to measure the conductivity.

9.2.4.2 Transference number measurement

The contribution of ions to conductivity is proved by transference number measurements which was carried out by placing the electrolyte (1g PVA: 0.75g PGSU: 0.6g NH_4SCN) of highest conductivity between stainless steel electrodes. A constant DC potential of 1.5 V was applied to polarise the cell using Wagner's DC polarisation technique where the current was monitored as a function of time.

9.2.4.3 Configuration of proton conducting battery

The highest conducting polymer electrolyte sample was evaluated for its performance in proton conducting battery.

9.3 RESULTS AND DISCUSSION

9.3.1 Characterisation techniques

(i) Fourier transform infrared spectroscopy (FT-IR)

The FT-IR analysis was made to project the complexation that has occurred between PVA, PGSU and the dopant NH_4SCN of various concentrations (0.5g, 0.6g, 0.7g) and was investigated from the change in vibrational modes as shown in **Fig. 9.1**. Keen observation of the **Fig. 9.1(a)** revealed the bands corresponding to –OH stretching at 3296.23 cm^{-1} followed by >C=O stretching and –C-O-C- stretching linkages at 1700.05 cm^{-1} and 1043.81 cm^{-1} which was confined to poly(glycerol suberate) (PGSU). As per the report stated by **Premlatha *et al.,*** poly(vinyl alcohol) (PVA) experienced a peak at 3455 cm^{-1} pertaining to –OH stretching[43]. In addition two more peaks owing to $–CH_2-$ asymmetric stretching and >C=C< stretching were assigned to be at 2910 cm^{-1} and 1647 cm^{-1}. The FT-IR spectrum of polymer blend (PVA-PGSU) shown in **Fig. 9.1(b)** manifested a shift in peaks towards 3213.44 cm^{-1}, 1717.47 cm^{-1}, 1032.52 cm^{-1}, 2934.94 cm^{-1} corresponding to the –OH, >C=O, -C-O-C- and $–CH_2$ stretching vibrations of PVA and PGSU that could be evidenced for the possible blending between PVA and PGSU. In **Fig. 9.1(c-e)** bands related to $–CH_2$ stretching were found to be observed at 2946.23 cm^{-1}, 2954.86 cm^{-1} and 2923.65 cm^{-1} which has undergone a possible shift from 2934.94 cm^{-1}. New peaks elicited at 2052.41 cm^{-1}, 2051.81 cm^{-1} and 2052.98 cm^{-1} in **Fig. 9.1(c-e)** represented linkages of NH_4SCN as revealed by **Muthuvinayagam *et al.,***[21] owing to a confirmation that the added salt has dispersed well within the polymer matrix. Further the shifts related to –OH stretching assigned at 3246.21 cm^{-1}, 3233.35 cm^{-1} and 3190.86 cm^{-1} from 3213.44 cm^{-1} accompanied with the variation in intensity of the peaks suggested the complexing ability between polymer blend and the salt added[16]. The linkages attributed to >C=O stretching and >C-O-C< groups were shifted from 1717.47 cm^{-1} and 1032.52 cm^{-1} to the values as displayed in the **Table 9.1**. All these results favoured the possibility of interaction among all the additives as shown in **Fig. 3**.

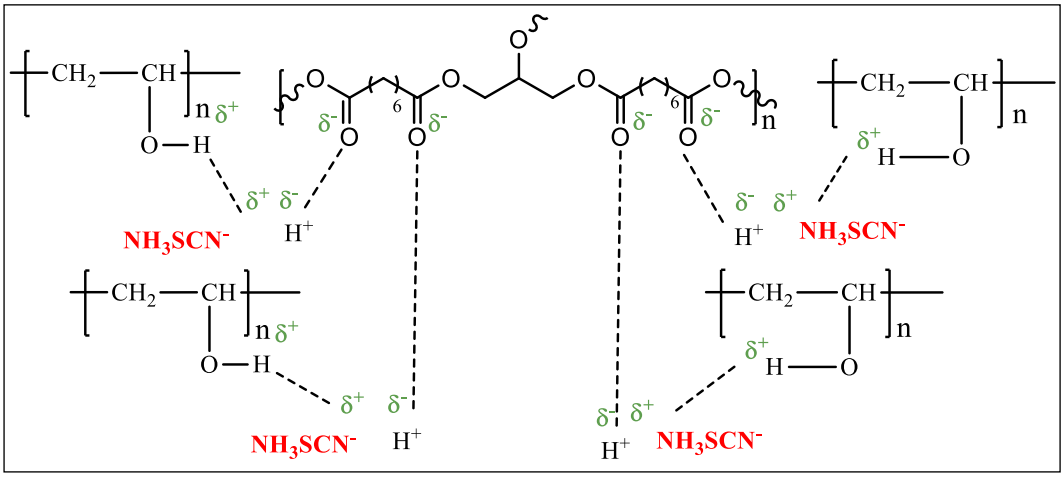

Fig. 3 Possible interaction between blend polymer (PVA+PGSU) and NH_4SCN

(ii) X-ray diffraction studies (XRD)

As a motto of determining the interaction within the polymer blend and between PVA-PGSU - NH_4SCN, XRD measurements were carried out followed by displaying the diffraction patterns in **Fig. 9.2(a-d)**. The XRD patterns in **Fig. 9.2(a)** shows peak, 2Θ at 19.10º which might be contributed to the crystalline nature of the polymer. Decrease in crystallinity can be obviously noticed in **Fig. 9.2(b-d)** which is resembled in the form of broadened peaks with relatively less intensity rendering amorphous nature that can facilitate the segmental motion of the polymer electrolyte as given by **Vinoth Pandi *et al.*,**[44]. This can be interpreted with the statement of **Hodge *et al.*,** who established a correlation between the intensity of the peak and the degree of crystallinity[45]. The complexing ability within the PVA-PGSU-NH_4SCN could be still evident on observing a shift from 2Θ = 19.10º of pure blend to higher Braggs angle of 22.50 º, 23.11º and 22.51º in doped systems[46]. Correlating the peaks pertaining to NH_4SCN (JCPDS No. 1762-95-4) as shown in the supplementary data of **Nirmala Devi *et al.*,**[47], no resemblance was observed in the salt doped pattern of the present investigation. Moreover the added dopant facilitates the changes in the amorphous hump which in turn disturbs the polymer blend to get interacted[14].

(iii) Differential scanning calorimetry (DSC)

Typical DSC thermograms of pure (1g PVA: 0.75g PGSU) and NH_4SCN (0.5g-0.7g) doped systems displayed in **Fig. 9.3(a-d)** can be viewed in detail to study the change in heat flow which is generally termed as glass transition temperature (T_g) taking place at a range of temperature where its midpoint is accompanied with maximum shift of heat flow considered as mean value of distribution[48]. It is a general representation that the addition of dopant

suppresses the T_g. But the present discussion elicits a T_g value of 84.54°C for pure blend which got successively increased to 116.50°C (0.5g), 122.35°C (0.6g), 182.21°C (0.7g) on adding NH_4SCN of various proportions as shown in **Table 9.2**. This enhanced T_g could be reasoned due to the preferable interaction of H^+ ions with electronegative atoms of polymer blend at multiple coordination sites[49] resulting in cross linkage that can reduce the pliability of the polymeric backbone which in turn hinders the rotation of polymer segments thereby inducing stiffness and elevating the energy barrier that retards the segmental motion[50]. It is noteworthy to relate the increase in T_g value with the report framed by **Ramaswamy *et al.,***[51] where increasing the dopant facilitates increased number of free charge carriers (H^+) providing a facile cross linkage between anions and cations.

(iv) Scanning electron microscopy (SEM) and Energy dispersive X-ray spectroscopy (EDS)

The SEM images incorporated with its elemental peaks for pure blend as well as the NH_4SCN doped systems can be seen in **Fig. 9.4**. **Fig. 9.4(a)** clearly predicted the uniform blend that has occurred between PVA and PGSU. However minute inhomogeneity observed may be due to micro immiscibility of the blend. **Fig. 9.4(b-d)** shows the dispersion of the added dopant NH_4SCN within the polymer electrolyte that could be seen in the form of fine flake appearance confirming the dispersion of salts. On examining the corresponding EDS spectra shown in **Fig. 9.4(a-d)** and data from **Table 9.3**, the absence of peaks corresponding to N and O in **Fig. 9.4(a)** and its presence along with C and O peaks in the **Fig. 9.4(b-d)** with increased intensity on increasing the concentration of dopants supported the same as revealed from SEM analysis. On the other hand decrease in intensity of C and O peaks in **Fig. 9.4(b-d)** may be due to the good blending nature with the added salt.

9.3.2 Conductivity measurements

9.3.2.1 AC impedance analysis

Fig. 9.5(a) represents the Cole-Cole plot of pure polymer electrolyte (1g PVA: 0.75g PGSU blend) followed by its doped systems in **Fig. 9.5(b)** with corresponding equivalent circuit. A complex plane impedance plot is generally associated with a semicircle (high frequency) due to the bulk effect of the electrolyte which is a parallel combination of bulk resistance and bulk capacitance and an inclined spike at low frequency due to electrode-electrolyte interface rendering a constant phase element (CPE). Here, the resistor represents the ionic migration through free polymer matrix whereas the capacitor indicates the immobile

polymer chains that could get polarised in an alternate field. The bulk resistance (R_b) can be elicited from the intercept of semicircle or low frequency spike on real axis ($Z^{|}$) from which the ionic conductivity can be evaluated using the below eq. 1,

$$\sigma = \frac{l}{R_b A} \text{Scm}^{-1} \qquad (1)$$

where σ is the ionic conductance, R_b is the bulk resistance, l and A are thickness and area of film.

From the **Fig. 9.5(a,b)**, it is obvious that the concentration of dopant is inversely related to the diameter of the semicircle. From the disappearance of the semicircle it is evident that, a non-capacitive nature has emerged due to the random orientation of polar side groups of polymeric network owing to a resistive component only[52]. The bulk resistance (R_b) was extracted from the Cole-Cole plot with the help of EQ software designed by **Boukamp**[53]. The derived EIS parameters are listed in the **Table 9.4**. From the table, it is evident that on increasing the concentration of dopant, R_b value has decreased from 1.6 x 10^5 ohm to 63.5 ohm corresponding to the composition (1g PVA: 0.75g PGSU: 0.6g NH_4SCN) possessing maximum conductivity of 3.01 x 10^{-4} Scm^{-1} which confirms that the conductivity is favoured by increased charge carriers[54]. It is noticeable that the ionic conductivity of pure PVA reported as 2.5 x 10^{-10} S/cm has increased in the present discussion[55]. This increased conductivity could be reasoned due to the changes in mobility and charge carrier concentration that can disrupt the bonding between the oxygen and its attached sites thereby creating more sites for facile proton ion (H^+) interaction resulting in continuous hopping of H^+ ions through the co-ordination sites rendering highest conductivity as stated by **Monisha *et al.,***[50]. Except the three tightly bound hydrogen atoms of NH_4^+, the fourth weakly bound H^+ ion has the capability of getting dissociated under the electric field thereby initiating the proton conduction mechanism. Increased amorphous nature revealed from XRD measurements, increase the number of transit sites, the possible interaction shown in FT-IR and **Fig. 3** also supports the same. On the other hand, when the concentration of the dopant exceeded 0.6g, the conductivity was found to decrease to 9.02 x 10^{-5} Scm^{-1} though there is an increase in the number of charge carriers. This might be due to some factors like ionic agglomeration leading to ion pairs or ion triplets, charge cloud effect or reduced chain mobility which is evident from its bulk resistance, R_b (184.3 ohms) as supported by **Leena Chandra *et al.,***[56].

9.3.2.2 Conductance spectra

Fig. 9.6 represents the frequency dependence of AC conductivity for pure blend (1g PVA: 0.75g PGSU) as well as different proportions of NH_4SCN doped electrolytes. Generally a conductance spectra comprises of three regions where the low frequency dispersion region indicates the space charge polarisation at blocking electrodes, the mid free portion indicates plateau region owing to the dc conductivity (σ_{dc}) of the system and the high frequency region is due to the bulk relaxation process as a result of columbic interaction of charge carrier and disorder within the structure[57]. In this case, two well defined regions observed for doped systems are absent in pure polymer electrolyte. The low frequency dispersion region was attributed to the ion blockage at electrode-electrolyte interface and the mid frequency flat region correspond to the bulk conductivity[58,59]. The measured dc conductivity obtained by extrapolating the flat region to zero frequency was in good agreement with the values obtained from Cole-Cole plots. At low frequency, conductance is high due to the accumulation of charges at electrode, whereas at high frequency the applied field duration is short making charging process slower thereby making the ac conductivity a frequency independent value equal to dc conduction.

9.3.2.3 Dielectric spectra analysis

To study the relaxation of dipoles within the polymer electrolyte, dielectric analysis was made which is generally ascribed by the complex permittivity ε* using the equation,

$$\varepsilon^* = \varepsilon'(\omega) - i\,\varepsilon''(\omega)$$

where ε’ (ω) and ε’’(ω) are the real and imaginary parts corresponding to storage and loss of energy in each cycle of applied electric field[60].

Fig. 9.7(a,b) shows the plot corresponding to the frequency dependent ε’(ω) and ε’’(ω) for pure blend and salt doped systems at room temperature. The charge stored in a material and its dissipation are termed as dielectric constant (ε’) and dielectric loss (ε’’). From the plots, it is found that ε’and ε’’ increased at low frequency as a result of electrode polarisation, space charge effects confirming non-Debye behaviour of the electrolytes[61]. But at high frequency region, periodic reversal of the electric field disabled the ions from orienting themselves according to the direction of the electric field resulting in accumulation of trapped ions at electrode-electrolyte interface leading to decreased ε’and ε’’. On increasing the concentration of dopant to 0.7g, a decrease in dielectric constant was observed similar to conductivity measurements[62].

9.3.2.4 Modulus analysis

The dielectric behaviour of polymer electrolyte can be discussed on the basis of electrical modulus studies. Complex electrical modulus (M*) can be deduced from complex dielectric constant ($\varepsilon^{'}$) using the below relationship,

$$M^* = \frac{1}{\varepsilon'} = M' + jM'' \qquad (2)$$

where M' & M'' refers real and imaginary part of electrical modulus.

Modulus spectra (M vs log f) shown in **Fig. 9.8(a,b)** exhibit the variation of M' and M'' with frequency for doped and undoped systems. Both the plots pointed modulus towards zero at low frequency which is an indication that the electrode polarisation effect has been suppressed[63]. At high frequency, modulus gradually increased indicating the bulk effect of the material insisting polymer electrolytes to be ionic conductors. Also increased value of M'' can favour the hopping of ions between the sites of even long distance. The long tail appearance at low frequency confirmed non-Debye behaviourance due to large capacitance values within electrodes[64].

9.3.2.5 Transference number

Transference number measurements based on Wagner's polarisation technique predicts the domination of the conducting species ie., either ion or electrons. The initial current (I_i) was noted at the moment when a constant dc voltage of 1.5 V is supplied to the electrolyte. As time proceeded, the current gradually decreased and became stable when the polarisation was terminated paving way for the measurement of final current (I_f). From the initial and final current, the transference number of ion and electron were derived using the below equation,

$$t_+ = \frac{I_i - I_f}{I_i} \qquad (3)$$

$$t_{ele} = \frac{I_f}{I_i} \qquad (4)$$

where t_+, t_{ele}, I_i and I_f represents transference number of cation and electron, initial and final current.

From the parameters listed in **Table 9.5**, it is found that t_+ (0.9773) was profoundly increased than t_{ele} (0.0226) insisting that the conductivity is mainly contributed by the ions rather than the electrons[65,66]. This is additionally evident from the statement given by **Yap** [67] where the ionic conductor is ever accompanied by a rapid drop of current with time which could not be observed in case of non-ionic conductor. Similar pattern is noticed in **Fig. 9.9**, plot of current versus time where a saturation could be seen. Electrolyte film comprises of different ions possessing various mobility that can contribute towards the total current[68]. Though both the cations and anions have the capability of moving, it is highly specific to deal with cationic transference number (t_+) since it is mainly responsible for intercalation – de-intercalation processes at cathode during charging-discharging cycle in batteries[69]. However the performance of a polymer electrolyte can be assessed by means of transport parameters such as number of mobile ions(n) and mobility (μ)[70] which can be derived from the following expressions,

$$n = N\rho \times \text{molar ratio of salt} / \text{molecular weight of salt}$$

where n - no. of charge carriers depending on salt concentration

N – Avogadro number

ρ – density of salt

$$\mu = \mu_+ + \mu_- = \frac{\sigma}{ne}$$

$$t_+ = \frac{\mu_+}{\mu_+ + \mu_-} \qquad (5)$$

where μ, μ_+ and μ_- represents total, cationic and anionic mobility.

From the following equation, the diffusion co-efficient of cations and anions can be elicited.

$$D_+ + D_- = \frac{KT\sigma}{ne^2}$$

$$t_+ = \frac{D_+}{D_+ + D_-}$$

where K-Boltzmann constant

T- absolute temperature

σ – conductivity

e – charge of electron

D_+, D_- are the diffusion co-efficient of cation and anion

From the display of these parameters in **Table 9.5**, the cationic mobility ($\mu_+ = 5.071 \times 10^{-6}$ $cm^2 V^{-1}S^{-1}$) greater than anionic mobility ($\mu_- = 0.118 \times 10^{-6}$ $cm^2V^{-1}S^{-1}$) validated that, the conduction phenomena is due to cation that coincides well with the diffusion co-efficient ($D_+ > D_-$). From this measurement it is inferred that the H^+ ion being smaller in size could get possibly attached through hydrogen bonding thereby limiting the mobility of larger ions where the diffusion as well as mobility influences the ionic conductivity[71].

9.3.2.6 Configuration of proton conducting battery

(i) Preparation of anode and cathode

To configure a proton conducting battery, anode was prepared by mixing Zinc(metal) powder, $ZnSO_4.7H_2O$ and graphite in the ratio of 3:1:1 followed by the preparation of cathode by grinding desired proportion of V_2O_5, PbO_2, graphite and highest conducting polymer electrolyte (1g PVA + 0.75g PGSU + 0.6g NH_4SCN) sample separately. The grounded mixture was then pelletized with the aid of hydraulic press. Graphite was introduced in both cathode and anode to induce electronic conductivity, whereas the added polymer electrolyte could reduce electronic polarisation[72]. To start with, the highest conducting polymer electrolyte was sandwiched between the prepared electrodes under teflon surroundings resulting in the following representation.

Zn (metal) + $ZnSO_4.7H_2O$ | 1g PVA + 0.75g PGSU + 0.6g NH_4SCN | V_2O_5 + PbO_2

(ii) Cell reaction and discharge characteristics

The above configured cell set up can undergo anode and cathode reaction as shown below,

Anode reaction : $Zn \longrightarrow Zn^{2+} + 2e^-$

Cathode reaction : $PbO_2 + 4H^+ + 2e^- \longrightarrow Pb^{2+} + 2H_2O$

$V_2O_5 + 6H^+ + 2e^- \longrightarrow 2VO^{2+} + 3H_2O$

As a result of cell reaction, it is expected to provide a voltage of $E_o = 2.2168$ V as the theoretical oxidation and reduction potential of Zn and PbO_2 are found to be - 0.7618 V and 1.455 V [73].

But when the schematic set up of the above cell as shown in **Fig. 9.10** was connected to a multimeter to measure open circuit voltage (OCV), it experienced a stabilised voltage of 1.51 V for a time period of 75 hours as displayed in **Fig. 9.11**. However the observed voltage was lesser than the expected voltage which could be attributed due to the possible reduction of $ZnSO_4.7H_2O$ at anode[74]. When an external load of 1MΩ was connected to study the discharge characteristics of the cell at room temperature, a drop in OCV was noticed from 1.51 V to 1.46 V as shown in **Fig. 9.12**, that could be reasoned due to the activation polarisation which would have occurred due to the controlled electrochemical reaction taking place on the electrode surface[75]. The observed drop to 1.46 V was stable up to 70 hours. This stable flat region was termed as plateau region beyond which it began to decrease. The obtained cell parameters displayed in **Table 9.6**, ensured that the prepared polymer electrolyte film is a promising potential source in solid state energy storage devices.

9.4 CONCLUSIONS

(i) A new blend polymer electrolyte based on PVA, poly(glycerol suberate) polyester (PGSU) doped with different amount of NH_4SCN was prepared.

(ii) FT-IR, XRD and DSC techniques revealed the complexation, amorphous nature and chain flexibility taking place within the polymer electrolyte.

(iii) SEM-EDS images clearly portrayed the dispersion of ammonium thiocyanate.

(iv) Highest ionic conductivity of 3.01×10^{-4} Scm^{-1} was observed for the optimised electrolytic film (1g PVA + 0.75g PGSU + 0.6g NH_4SCN) at room temperature.

(v) Non-Debye nature of the electrolyte film was revealed from dielectric and modular studies.

(vi) The observed cationic transference number close to unity proved conduction due to ion rather than electrons.

(vii) Electrolyte applied for battery was found to be stable up to 70 hours with 1.46 V under 1M Ω load.

9.5 REFERENCES

1. L. Long, S. Wang, M. Xiao, Y. Meng, J. Mater. Chem. A., **4** (2016) 10038–10069.
2. Jeffrey W. Fergus, J. Power Sources., **195** (2010) 4554–4569.
3. L. Porcarelli, C. Gerbaldi, F. Bella, J.R. Nair, Sci. Reports., (2016) 1-14.
4. J. Chai, Z. Liu, J. Ma, J. Wang, X. Liu, H. Liu, J. Zhang, G. Cui, L. Chen, Adv. Sci ., **4(1600377)** (2017) 1-9.
5. E. A. SECCO, Solid State Ionics – Materials and Applications, World Scientific, Singapore, (1992).
6. M.B. Armand, J.M. Chabagno, M. Duclot, Fast Ion Transport in Solids : Electrodes and Electrolytes, North Holland, NY, (1979).
7. M. Kumar, S.S. Sekhon, Eur. Polym. J., **38** (2002) 1297- 1304.
8. X. Qian, N. Gu, Z. Cheng, X. Yang, S. Wang, S. Dong, Mater. Chem. Phys., **74** (2002) 98-103.
9. R.C. Agrawal, G.P. Pandey, J. Phys. D: Appl. Phys., **41** (2008) 1-18.
10. P. Zhang, L.C. Yang, L.L. Li, M.L. Ding, Y.P. Wu, R. Holze, J. Membrane Sci., **379** (2011) 80-85.
11. D. Kumar, S.A. Hashmi, J. Power Sources, **195** (2010) 5101–5108.
12. S. Ferrari, E. Quartarone, P. Mustarelli, A. Magistris, M. Fagnoni, S. Protti, C. Gerbaldi, A. Spinella, J. Power Sources., **195** (2010) 559-566.
13. A.E. Steck, C. Stone, Proceedings of the Second International Symposium on New Materials for Fuel Cell and Modern Battery Systems, (1997).
14. N. Rajeswari, S. Selvasekarapandian, C. Sanjeeviraja, J. Kawamura, S. Asath Bahadur, Polym. Bull., **71(5)** (2014) 1061-1080.
15. Y. Liu, S. Gorgutsa, C. Santato, M. Skorobogatiy, J. Electrochem. Soc., **159(4)** (2012) A349-A356.
16. F.K.M. Genova, S. Selvasekarapandian, S. Karthikeyan, N. Vijaya, S. Sivadevi, C. Sanjeeviraja, . Polym plast technol Eng., **55(1)** (2016) 25-35.
17. V. Parameswaran, N. Nallamuthu, P. Devendran, E.R. Nagarajan, A. Manikandan, Physica B: Condensed Matter., **515** (2017) 89-98.
18. S. Thayumanasundaram, V.S. Rangasamy, J. WonSeo, J.P. Locquet. Electrochim. Acta., **240** (2017) 371-378.
19. R. Manjuladevi, M. Thamilselvan, S. Selvasekarapandian, R. Mangalam, M. Premalatha, S. Monisha, Solid State Ionics., **308** (2017) 90-100.

20. A. Alakanandana, A.R. Subrahmanyam, J. Siva Kumar, materialstoday: proceedings., **3(10)** (2016) 3680-3688.
21. M. Muthuvinayagam, C. Gopinathan, Polym., **68** (2015) 122-130.
22. M.J. Uddin, P.K. Alaboina, L. Zhang, S.J. Cho, Mater. Sci. Eng., B **223** (2017) 84-90.
23. Chun-ChenYang, J. Power Sources., **109(1)** (2002) 22-31.
24. Y. Ma, L.B. Li, G.X. Gao, X.Y. Yang, Y. You, Electrochim. Acta., **(187)** (2016) 535-542.
25. J. Chatterjee, T. Liu, B. Wang, J.P. Zheng, Solid State Ionics., **181(11–12)** (2010) 531-535.
26. X. Ma, X. Huang, J. Gao, S. Zhang, Z. Deng, J. Suo, Electrochim. Acta., **115** (2014) 216-222.
27. A. Awadhia, S.K. Patel, S.L. Agrawal, Prog. Cryst. Growth Charact. Mater., **52(1-2)** (2006) 61-68.
28. N.R. Chodankar, D.P. Dubal, A.C. Lokhande, C.D. Lokhande, J. Colloid Interface Sci., **460** (2015) 370-376.
29. Chun-ChenYang, Sheng-Jen Lin, J. Power Sources., **112(2)** (2002) 497-503.
30. J. Qiao, J. Fu, R. Lin, J. Ma, J. Liu, Polym., **51(21)** (2010) 4850-4859.
31. P. Tamilselvi, M. Hema, Physica B: Condens. Matter., **437** (2014) 53-57.
32. G. Merle, S.S. Hosseiny, M. Wessling, K. Nijmeijer, J. Membr. Sci., **409-410** (2012) 191-199.
33. G.M. Wu, S.J. Lin, C.C. Yang, J. Membr. Sci., **280(1-2)** (2006) 802-808.
34. Q. Wu, J. Zhang, S. Sang, J. Phys. Chem. Solids., **69(11)** (2008) 2691-2695.
35. A.L. Saroj, R.K. Singh, J. Phys. Chem. Solids., **73(2)** (2012) 162-168.
36. G.M. Wu, S.J. Lin, C.C. Yang, J. Membr. Sci., **275(1-2)** (2006) 127-133.
37. Chiam-WenLiew, S. Ramesh, A.K. Arof, Int. J. Hydrogen Energy., **39(6)** (2014) 2917-2928.
38. O.G. Abdullah, S.B. Aziz, M.A. Rasheed, Res. Phys., **6** (2016) 1103-1108.
39. C.W. Liew, S. Ramesh, A.K. Arof, Int. J. Hydrogen Energy., **39(6)** (2014) 2953-2963.
40. S. Sang, J. Zhang, Q. Wu, Y. Liao, Electrochim. Acta., **52(25)** (2007) 7315-7321.
41. H. Aydın, M. Şenel, H. Erdemi, A. Baykal, M. Tülü, A. Ata, J. Power Sources., **196(3)** (2011) 1425-1432.
42. J. Li, K. Lian, Polym., **99** (2016) 140-146.
43. M. Premalatha, N. Vijaya, S. Selvasekarapandian, S. Selvalakshmi, Ionics., **22(8)** (2016) 1299-1310.

44. D. Vinoth Pandi, S. Selvasekarapandian, R. Bhuvaneswari, M. Premalatha, S. Monisha, D. Arunkumar, K. Junichi, Solid State Ionics., **298** (2016) 15–22.
45. R.M. Hodge, G.H. Edward, G.P. Simon, Polym., **37** (1996) 1371–1376.
46. M. Premalatha, T. Mathavan, S. Selvasekarapandian, S. Monisha, D.Vinoth Pandi, S. Selvalakshmi, J. Non-Cryst. Solids., **453** (2016) 131–140.
47. G. Nirmala Devi, S. Chitra, S. Selvasekarapandian, M. Premalatha, S. Monisha, J. Saranya, Ionics., **23(12)** (2017) 3377-3388.
48. S. Selvalakshmi, N. Vijaya, S. Selvasekarapandian, M. Premalatha, J. Appl. Polym. Sci., **134(15)** (2017) 1-10.
49. M. Premalatha, T. Mathavan, S. Selvasekarapandian, S. Selvalakshmi, S. Monisha, Org. Electron. **50** (2017) 418-425.
50. S. Monisha, T. Mathavan, S. Selvasekarapandian, A.M.F. Beniala, G. Aristatilc, N. Manic, M. Premalatha, D. Vinoth pandi, Carbohydr. Polym., **157** (2017) 38–47.
51. M. Ramaswamy, T. Malayandi, S. Selvasekarapandian, J. Srinivasalu, M. Rangaswamy, Ionics., **23(7)** (2017) 1771-1781.
52. S. Monisha, S. Selvasekarapandian, T. Mathavan, A.M.F. Benial, S. Manoharan, S. Karthikeyan, J Mater Sci: Mater Electron., **27(9)** (2016) 9314-9324.
53. B.A. Boukamp, Solid State Ionics., **20** (1986) 31–44.
54. M. Ramaswamy, T. Malayandi, S. Selvasekarapandian, J. Srinivasalu, M. Rangaswamy, V. Soundararajan, Polym plast technol Eng., **56(9)** (2017) 992-1002.
55. V. Parameswaran, N. Nallamuthu, P. Devendran, E.R. Nagarajan, A. Manikandan, Physica B: Conden. Matter., **515** (2017) 89-98.
56. M. V. Leena Chandra, S. Karthikeyan, S. Selvasekarapandian, M. Premalatha, S. Monisha, J. Polym Eng., **37(6)** (2016) 617-631.
57. G. Boopathi, S. Pugalendhi, S. Selvasekarapandian, M. Premalatha, S. Monisha, G. Aristatil, Ionics., **23(10)** (2017) 2781-2790.
58. S. Selvasekarapandian, T. Savitha, J. Malathi, R. Mangalam, S.S. Ramya, Bionano-geo sciences: the future challenge, Ane Books Pvt Ltd, (2009).
59. A.K. Jonscher, J Mater Sci., **16** (1981) 2037–2060.
60. P. Dutta, S. Biswas, S.K. De, Mater Res Bull., **37** (2002) 193–200.
61. S. Ramesh, T.S. Yin, C.W. Liew, Ionics., **17** (2011) 705–713.
62. S. Ramesh, A.K. Arof, Mater Sci Eng., B **85** (2001) 11–15.
63. R. Richert, H. Wagner, Solid State Ionics., **105(1–4)** (1998) 167–173.
64. S. Ramesh, A. Yahaya, A. Arof, Solid State Ionics., **152** (2002) 291–294.

65. H.J. Woo, S.R. Majid, A.K. Arof, Mater. Res. Innovations., **15(s2)** (2011) s49-s54.
66. M.F. Shukur, M.F.Z. Kadir, Ionics., **21(1)** (2015) 111-124.
67. K.S. Yap, Characteristics of PMMA-grafted natural rubber polymer electrolytes, University of Malaya, (2012).
68. A. Ghosh, C. Wang, P. Kofinas, J. Electrochem. Soc., **157(7)** (2010) A846-A849.
69. A.K. Arof, N.E.A. Shuhaimi, S. Amirudin, M.Z. Kufian, H.J. Woo, M.A. Careem, Polym. Adv. Technol., **25(3)** (2014) 265-272.
70. S.R. Majid, A.K. Arof, Physica B: Condens. Matter., **355(1-4)** (2005) 78-82.
71. A.K. Arof, M.Z. Kufian, M.F. Syukur, M.F. Aziz, A.E. Abdelrahman, S.R. Majid, Electrochim. Acta., **74** (2012) 39-45.
72. S.M. Bansod, S.S. Bhoga, K. Singh, R.U. Tiwari, Ionics., **13(5)** (2007) 329-332.
73. N. Lakshmi, S. Chandra, J Power Sources., **108(1-2)** (2002) 256–260.
74. K. Mishra, D.K. Rai, J Korean Physical Soc., **62(2)** (2013) 311–319.
75. J. Broadhead, H.C. Kuo, In D. Linden, T. B. Reddy, Handbook of batteries, McGraw-Hill, (2001).

Table 9.1 FT-IR spectral assignments of PVA+PGSU+NH_4SCN blend polymer electrolytes

Composition	Assignments				
	-OH str (cm^{-1})	-C=O str (cm^{-1})	-C-O-C- str (cm^{-1})	$-CH_2$ str (cm^{-1})	$-C\equiv N$ (cm^{-1})
PGSU	3296.23	1700.05	1043.81	-	-
Pure (1g PVA: 0.75g PGSU)	3213.44	1717.17	1032.52	2934.94	-
Pure + 0.5g NH_4SCN	3246.21	1726.42	1019.35	2946.23	2052.41
Pure + 0.6g NH_4SCN	3233.35	1704.30	1051.81	2954.86	2051.81
Pure + 0.7g NH_4SCN	3190.86	1720.41	1055.40	2923.65	2052.98

Table 9.2 Glass transition temperature (T_g) of blend polymer electrolytes

Composition	T_g ^{o} (C)
Pure (1g PVA: 0.75g PGSU)	84.54
Pure + 0.5g NH_4SCN	116.50
Pure + 0.6g NH_4SCN	122.35
Pure + 0.7g NH_4SCN	182.21

Table 9.3 Elemental composition of synthesised blend polymer electrolytes

Composition	Element (Atomic weight %)			
	C	O	N	S
Pure (1g PVA: 0.75g PGSU)	64.21	35.79	-	-
Pure + 0.5 g NH_4SCN	56.09	29.32	13.22	1.37
Pure + 0.6 g NH_4SCN	53.89	24.36	19.99	1.76
Pure + 0.7 g NH_4SCN	52.11	23.04	22.97	1.88

Table 9.4 Ionic conductivity (σ) of PVA+PGSU+NH_4SCN blend polymer electrolytes at 303K

Composition	σ (Scm^{-1})	R_b (ohms)
Pure (1g PVA: 0.75g PGSU)	$7.77x10^{-8}$	$1.6x10^{5}$
Pure + 0.5g NH_4SCN	$6.68x10^{-5}$	246.4
Pure + 0.6g NH_4SCN	$3.01x10^{-4}$	63.5
Pure + 0.7g NH_4SCN	$9.02x10^{-5}$	184.3

Table 9.5 Transport parameters of NH_4SCN doped blend polymer electrolytes

Transport parameters	Composition
	Pure (1g PVA: 0.75 g PGSU) + 0.6 g NH_4SCN
t_+	0.9773
t_{ele}	0.0226
μ ($cm^2V^{-1}s^{-1}$)	$5.189x10^{-6}$
μ_+ ($cm^2V^{-1}s^{-1}$)	$5.071x10^{-6}$
μ_- ($cm^2V^{-1}s^{-1}$)	$0.118x10^{-6}$
D (cm^2s^{-1})	$1.355\ x10^{-7}$
D_+ (cm^2s^{-1})	$1.322\ x10^{-7}$
D_- (cm^2s^{-1})	$0.033\ x10^{-7}$

Table 9.6 Cell parameters for Pure (1g PVA: 0.75 g PGSU) + 0.6 g NH_4SCN blend electrolyte

Cell parameters	values
Cell area (cm^2)	1.1304
Cell weight (gm)	0.924
Cell diameter(cm)	1.2
Cell thickness (cm)	0.362
Open circuit voltage (V)	1.51

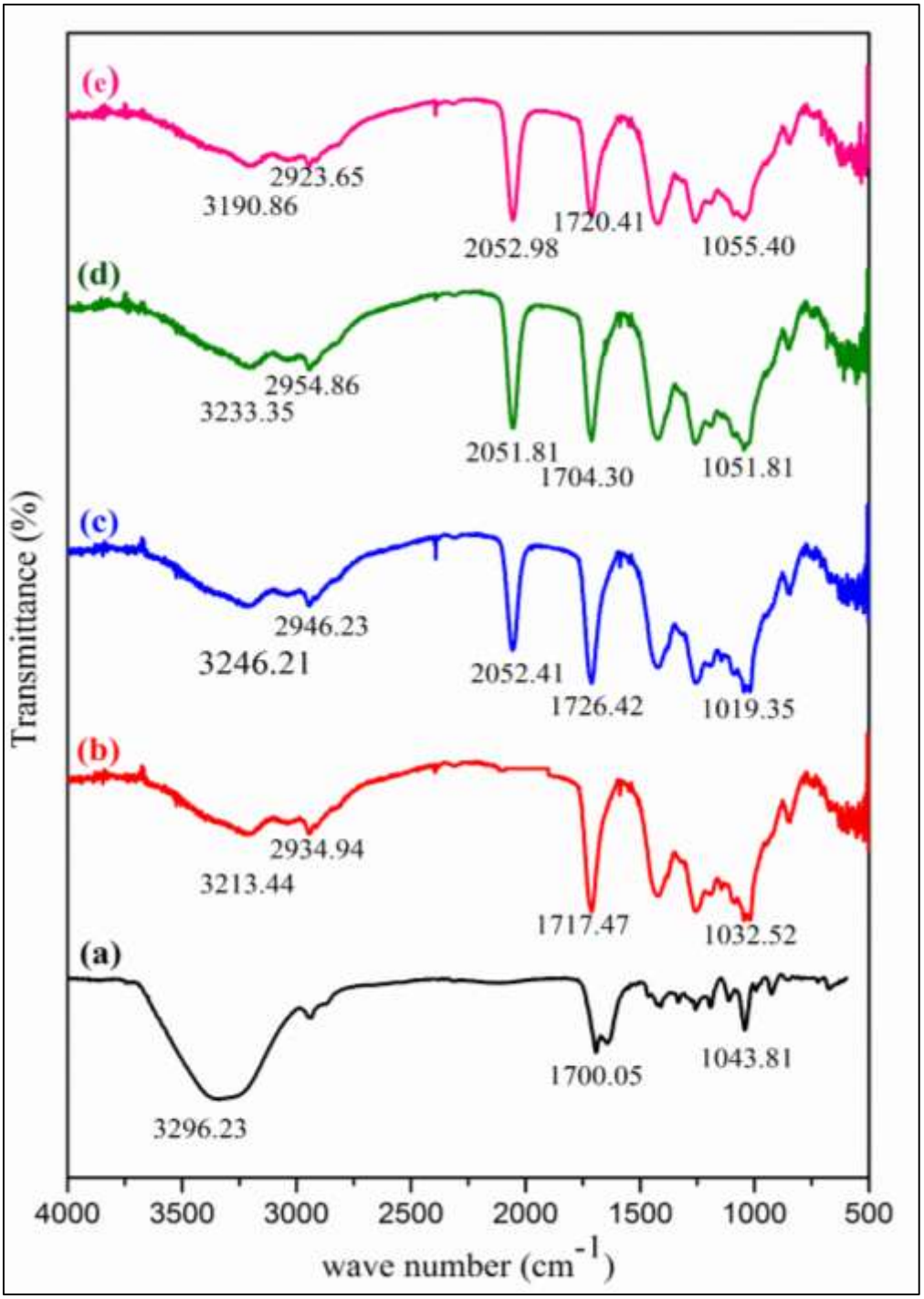

Fig. 9.1 FT-IR spectra of a) PGSU b) Pure (1g PVA: 0.75g PGSU) c) Pure + 0.5g NH_4SCN d) Pure + 0.6g NH_4SCN e) Pure + 0.7g NH_4SCN

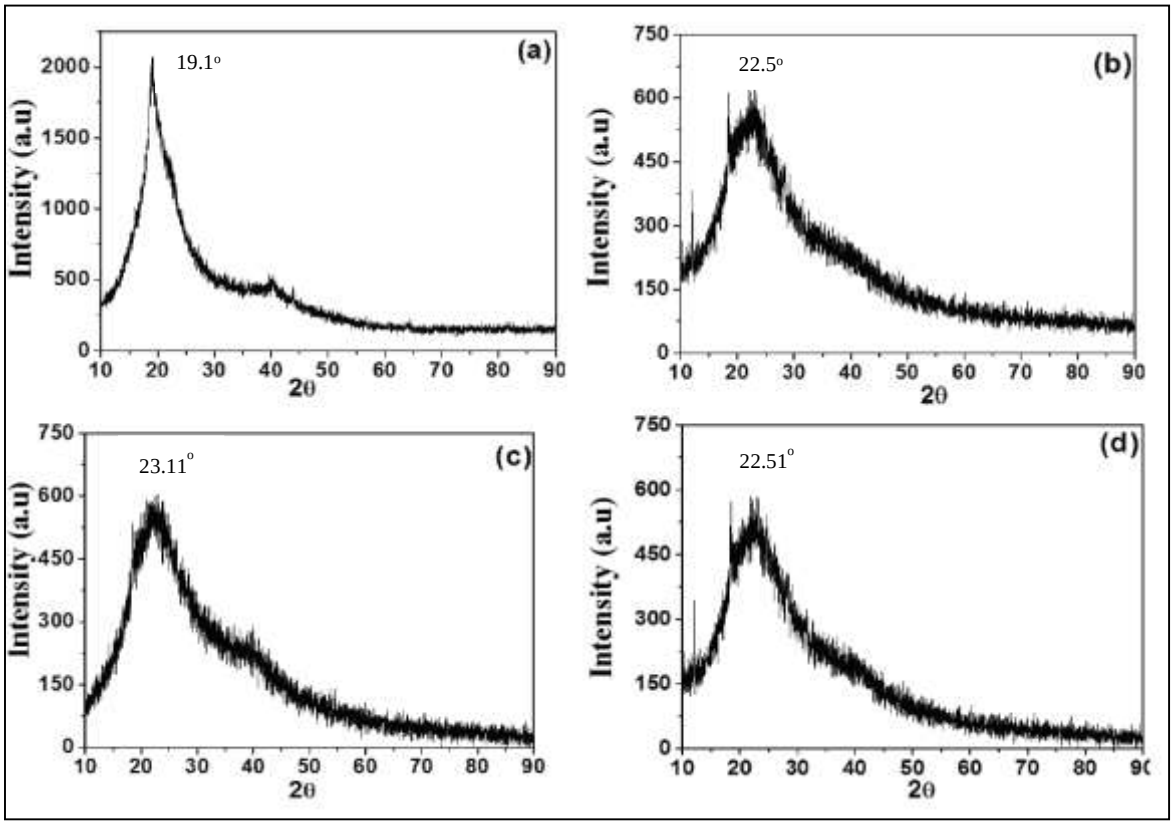

Fig. 9.2 XRD patterns of a) Pure (1g PVA: 0.75g PGSU) b) Pure + 0.5g NH_4SCN c) Pure + 0.6g NH_4SCN d) Pure + 0.7g NH_4SCN

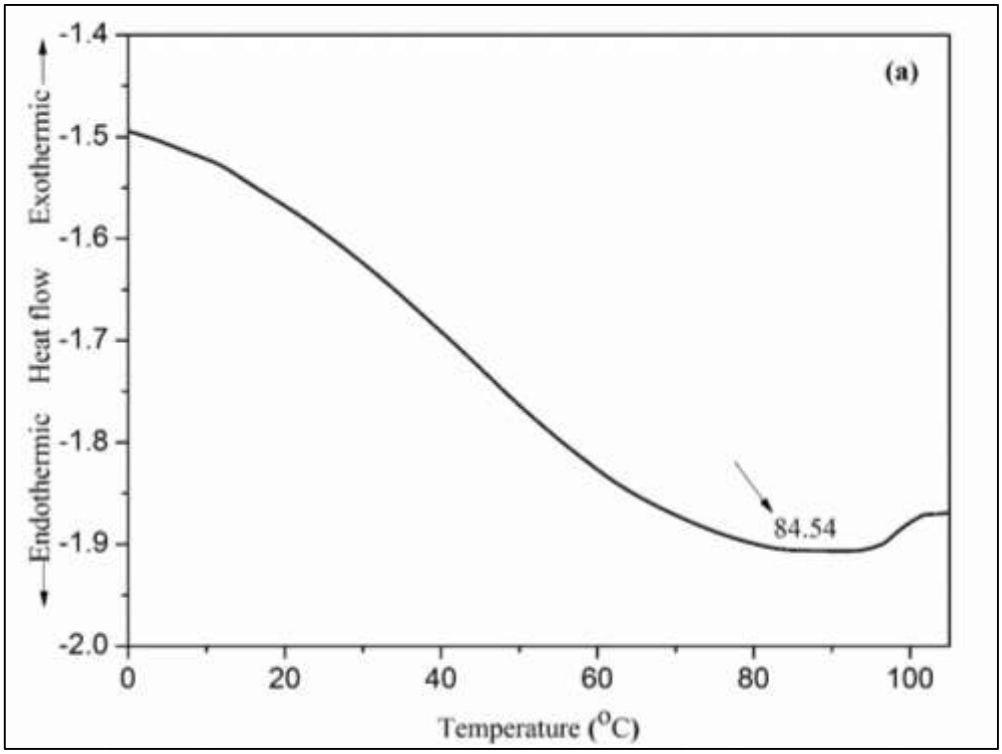

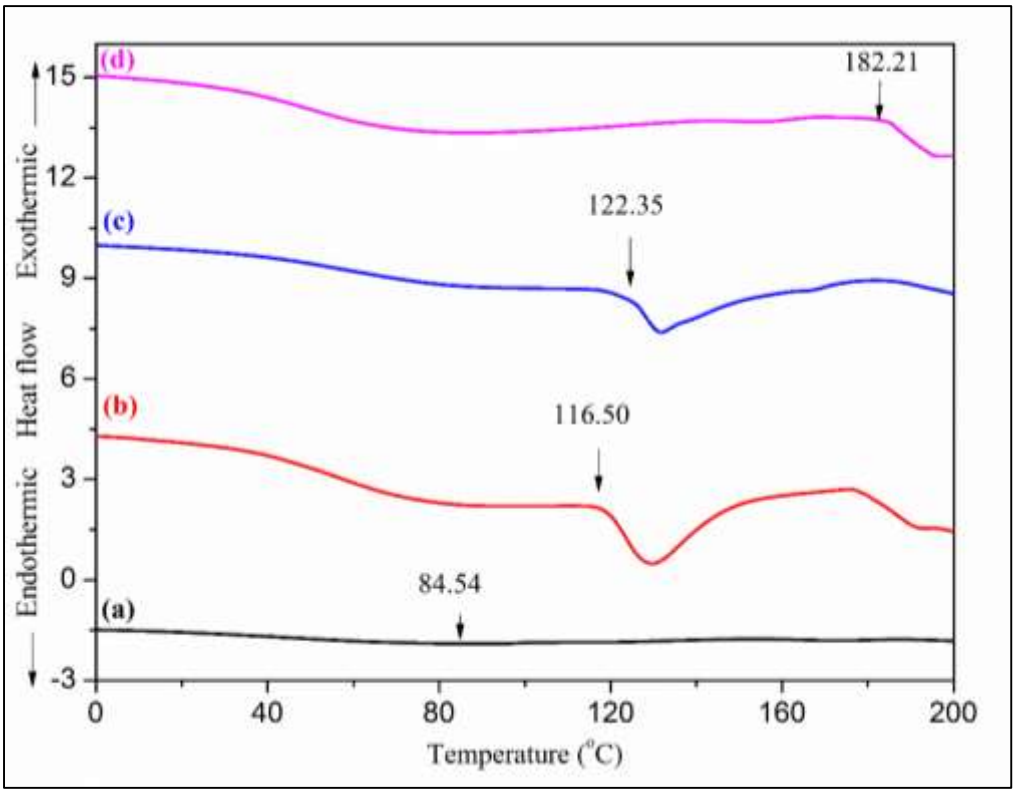

Fig. 9.3 DSC thermograms of a) Pure (1g PVA: 0.75g PGSU) b) Pure + 0.5g NH_4SCN c) Pure + 0.6g NH_4SCN d) Pure + 0.7g NH_4SCN

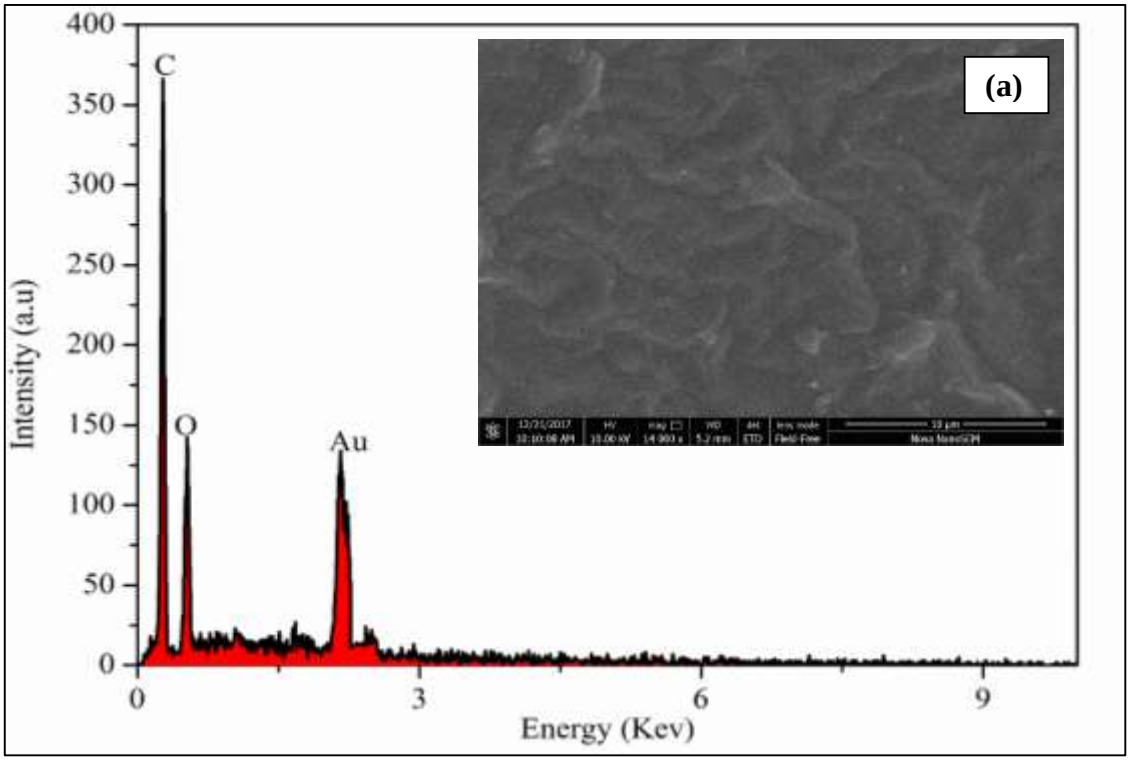
(a)
C
O
Au
Intensity (a.u)
Energy (Kev)
0
50
100
150
200
250
300
350
400
0
3
6
9

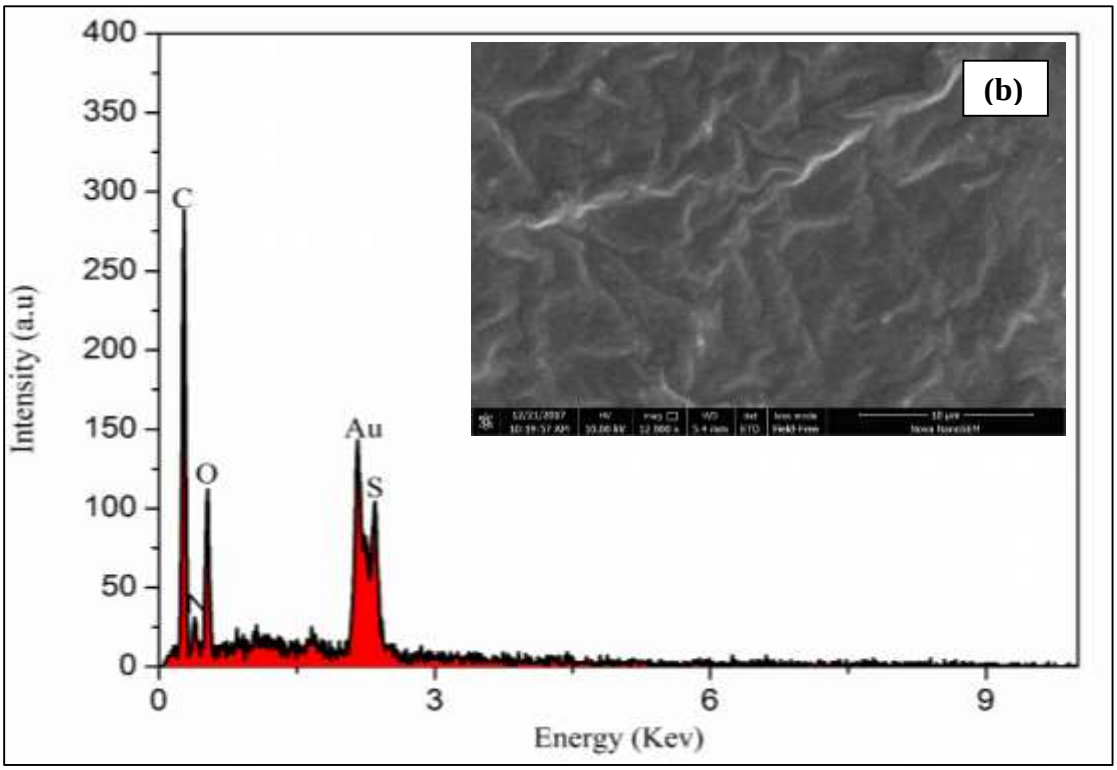
(b)
C
O
Au
S
Intensity (a.u)
Energy (Kev)
0
50
100
150
200
250
300
350
400
0
3
6
9

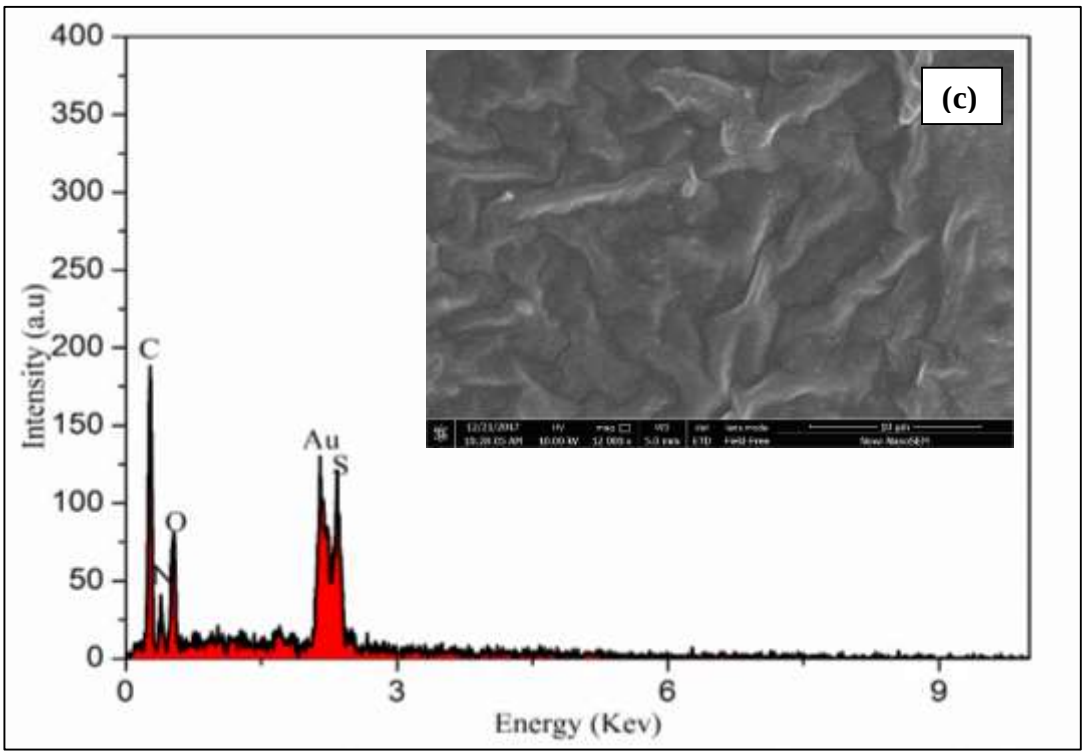

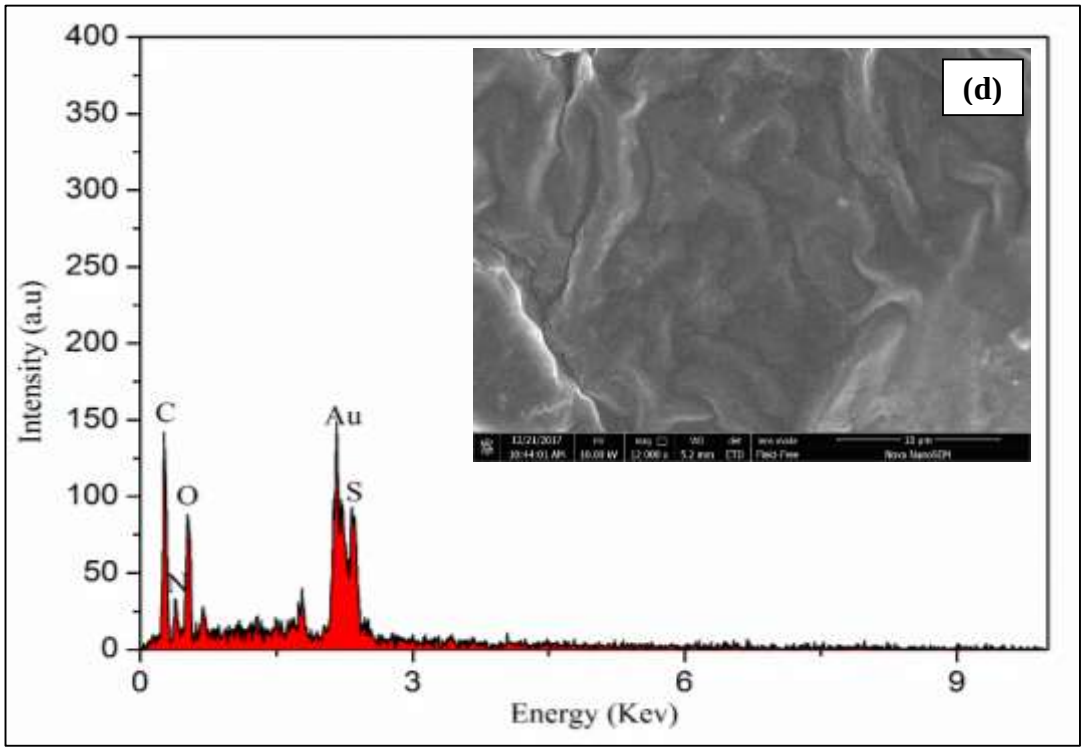

Fig. 9.4 Scanning electron microscopy (SEM) and Energy dispersive X-ray spectroscopy (EDS) images of a) Pure (1g PVA: 0.75g PGSU) b) Pure + 0.5g NH_4SCN c) Pure + 0.6g NH_4SCN d) Pure + 0.7g NH_4SCN

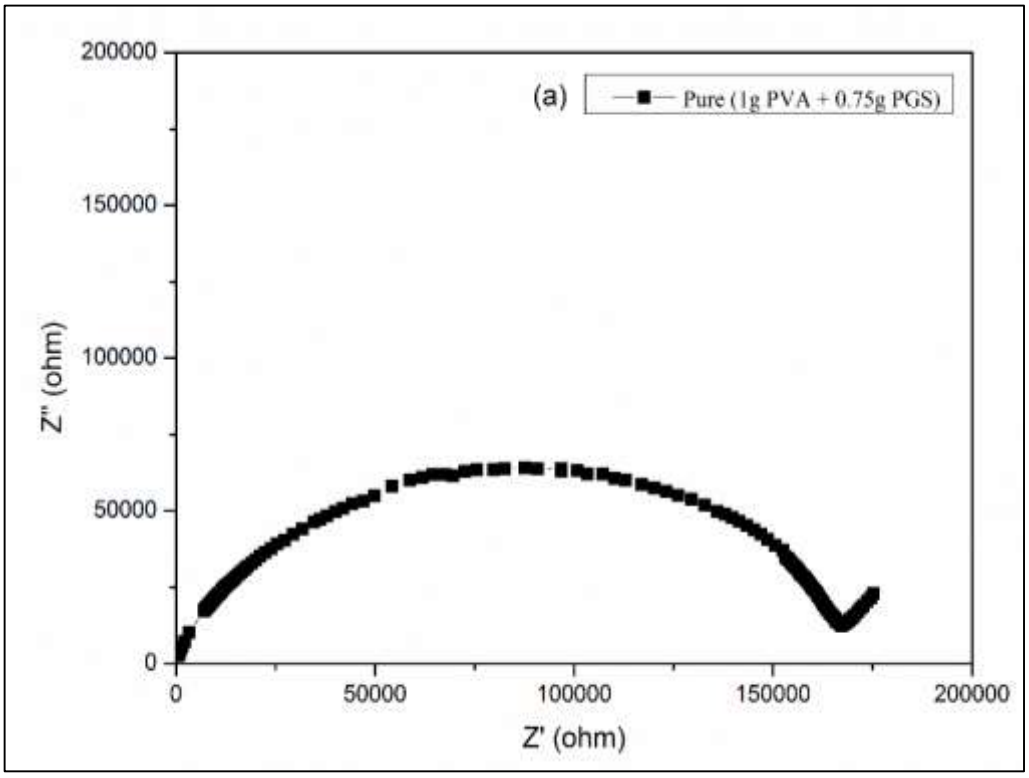

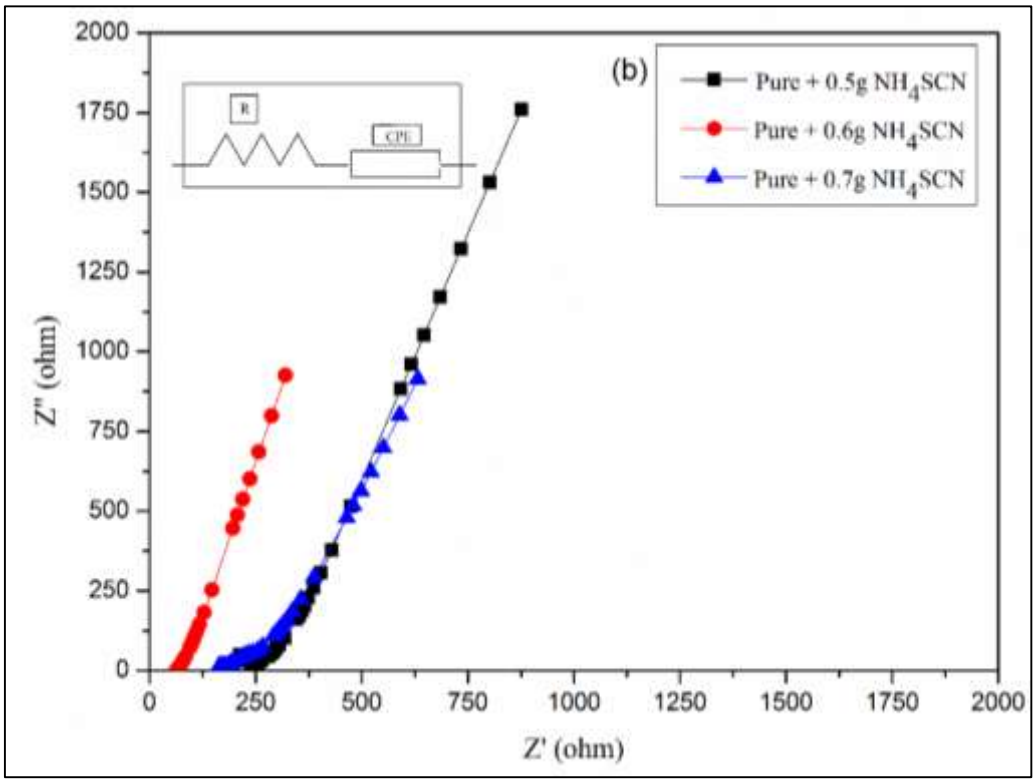

Fig. 9.5 Cole-Cole plots of a) Pure (1g PVA: 0.75g PGSU) b) Pure + 0.5g NH_4SCN, Pure + 0.6g NH_4SCN, Pure + 0.7g NH_4SCN

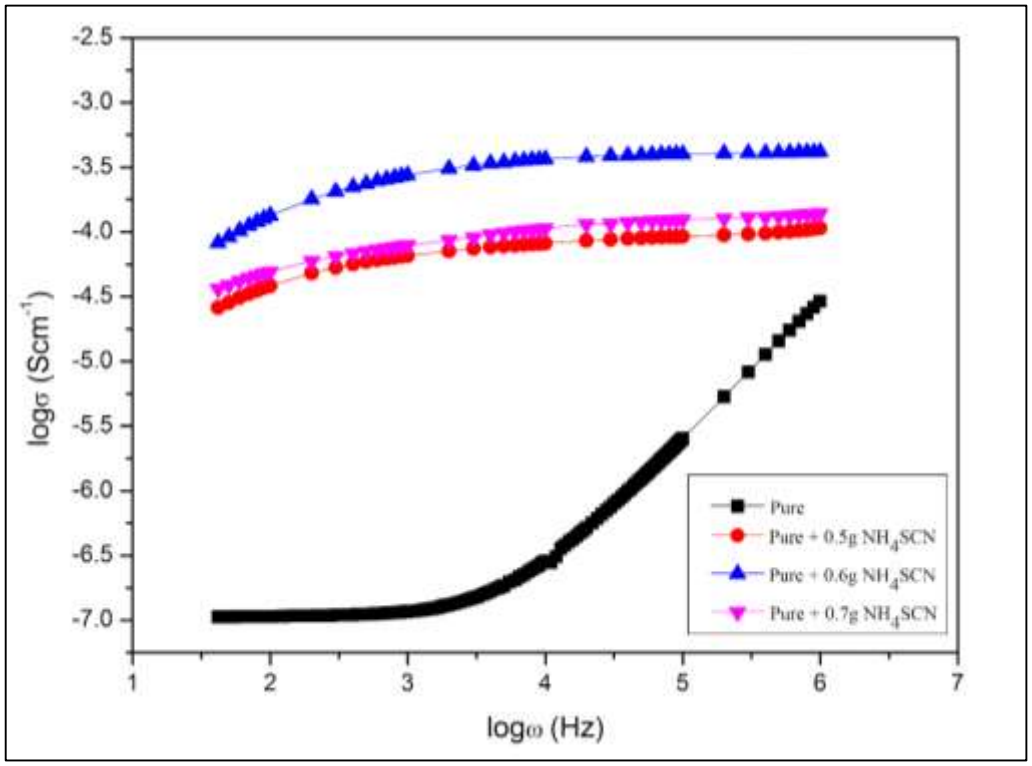

Fig. 9.6 Frequency (ω) dependence of conductivity (σ) for Pure and Pure doped with various concentrations of NH_4SCN

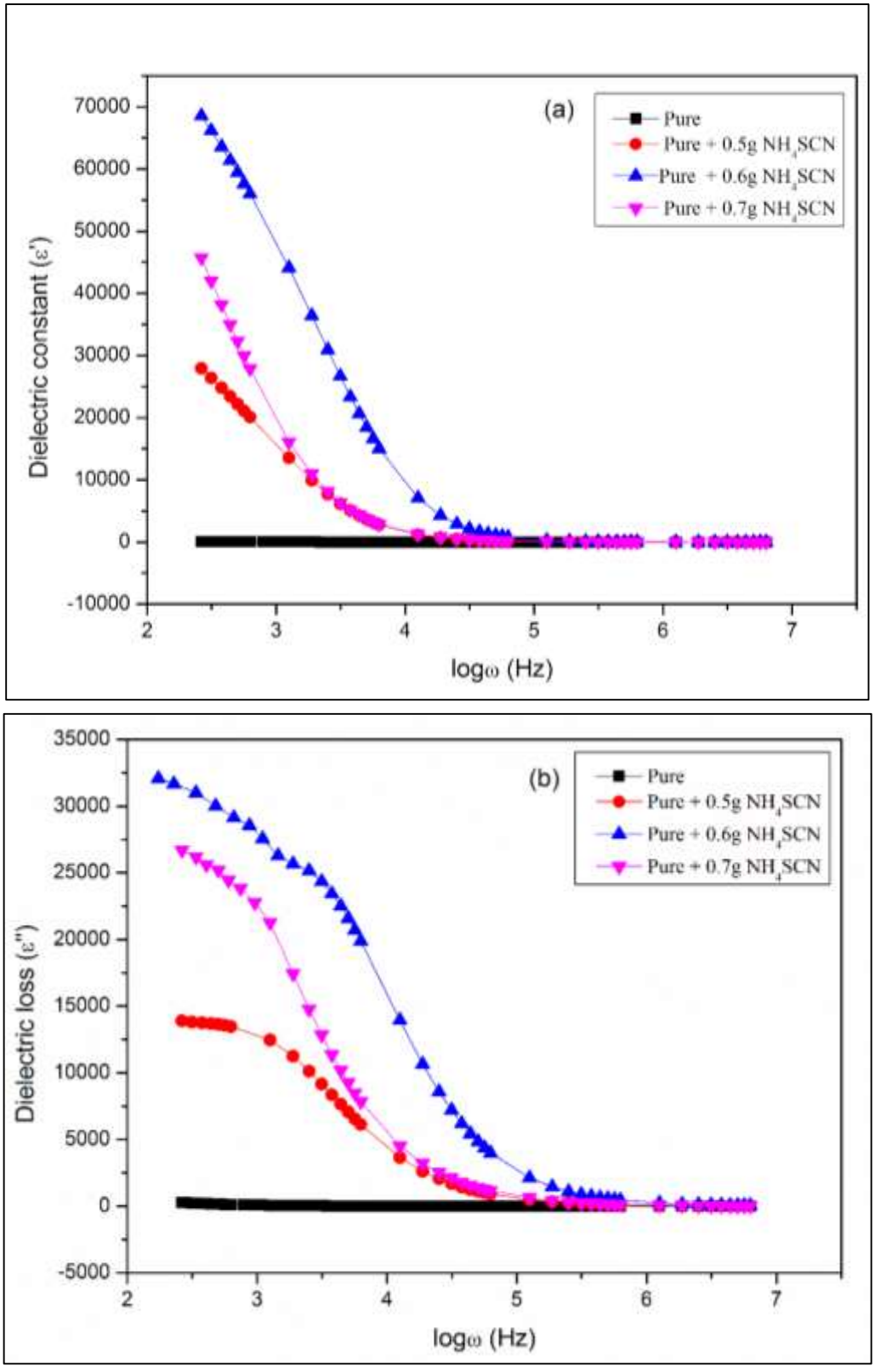

Fig. 9.7 (a,b) Frequency (ω) dependence of dielectric constant (ε') and dielectric loss (ε'') for Pure and Pure doped with various concentrations of NH_4SCN

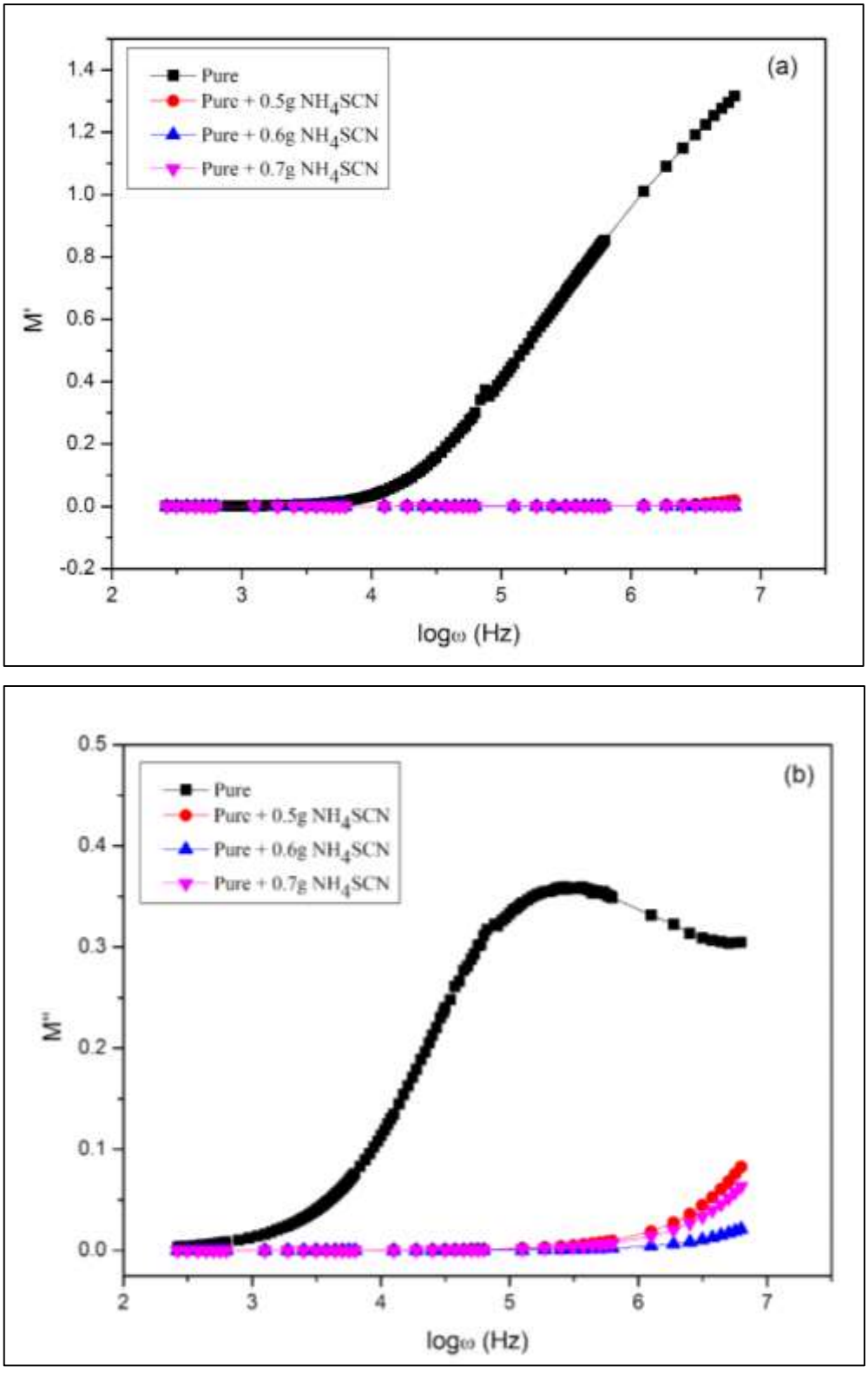

Fig. 9.8 (a,b) Frequency (ω) dependence of real (M') and imaginary (M'') modulus for Pure and Pure doped with various concentrations of NH_4SCN

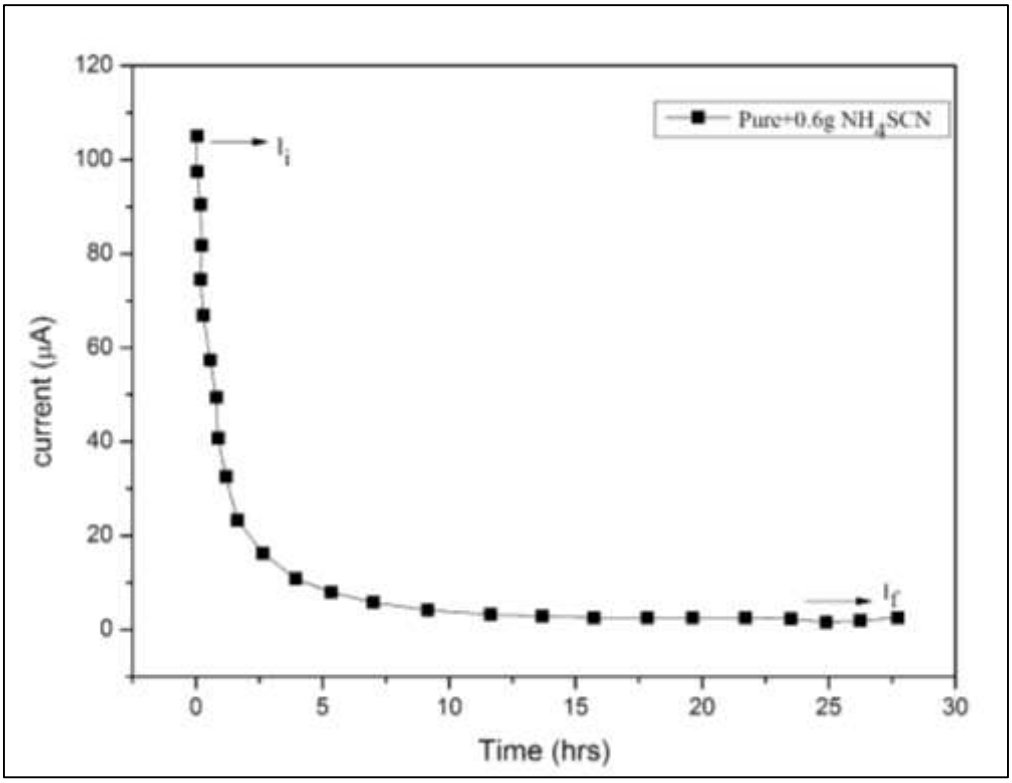

Fig. 9.9 Polarisation current vs time plot for Pure + 0.6g NH_4SCN

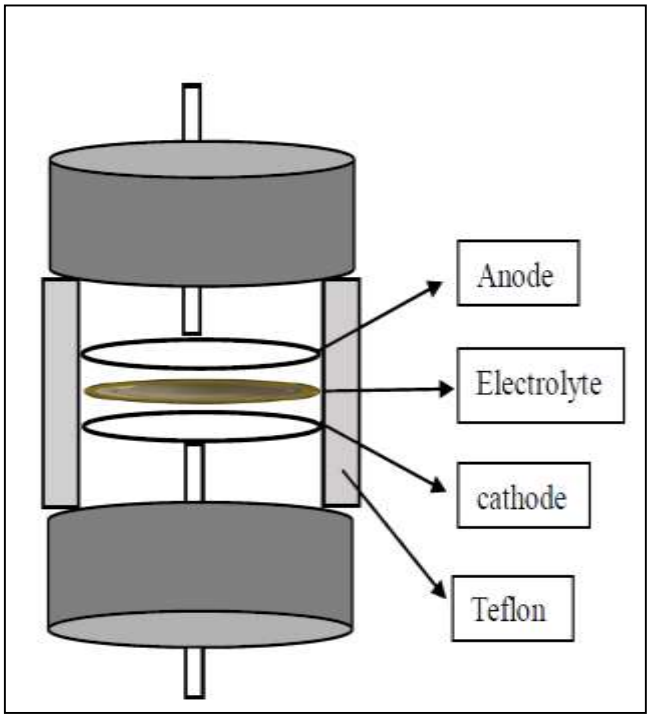

Fig. 9.10 Battery configuration

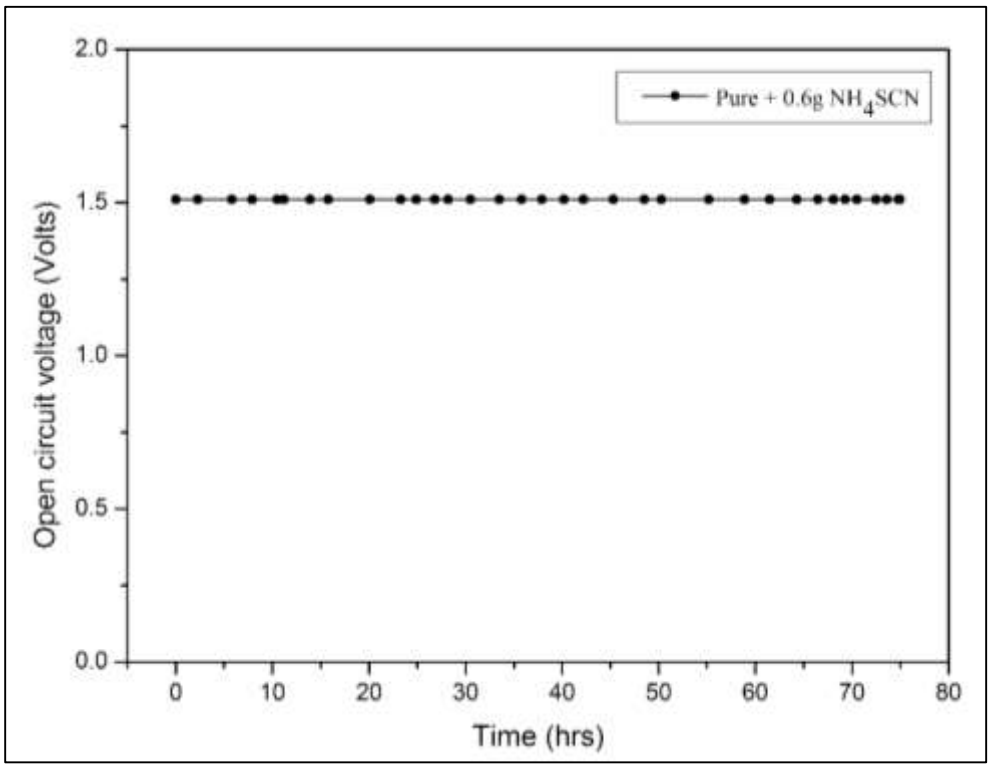

Fig. 9.11 Open circuit voltage Vs time plot for battery

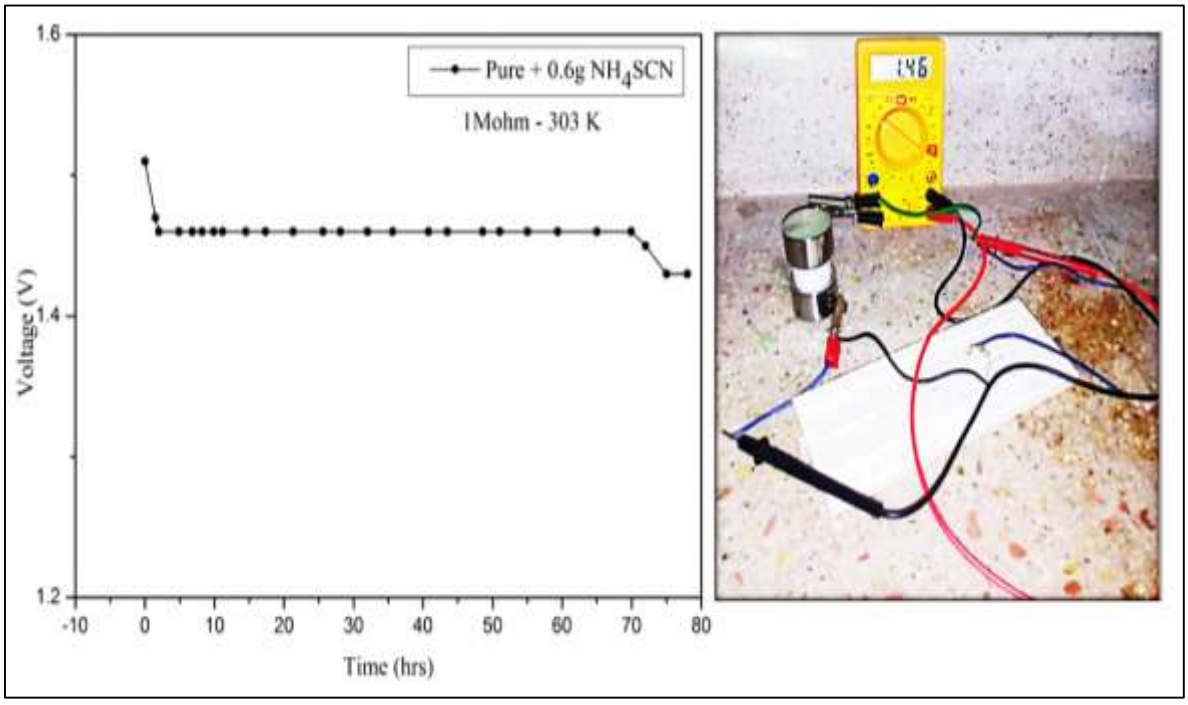

Fig. 9.12 Discharge curve for cell using 1 MΩ for 1g PVA + 0.75g PGSU + 0.6g NH_4SCN polymer electrolyte